Chapter 1
Nanoparticles: Preparation, Stabilization, and Control Over Particle Size

Maryam Razi, Maria Contreras-Mateus, Kotaybah W. Hashlamoun, and Nashaat N. Nassar

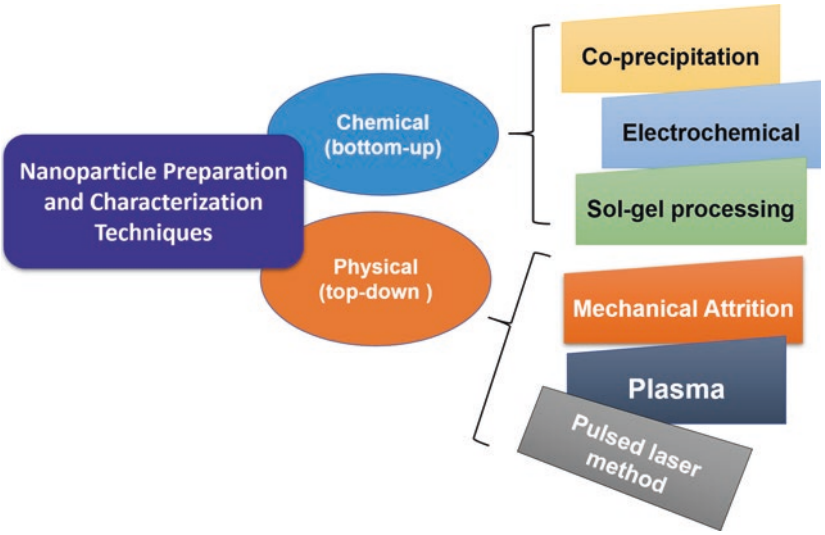

Graphical Abstract

1.1 Introduction

Human dreams often give rise to new science and technology. Nanotechnology, a twenty-first-century technology, was born out of these dreams. Nanotechnology is defined as the control and understanding of materials at scale between 1 and 100 nm,

M. Razi · M. Contreras-Mateus · K. W. Hashlamoun · N. N. Nassar (✉)
Department of Chemical and Petroleum Engineering, University of Calgary, Calgary, AB, Canada
e-mail: nassar@ucalgary.ca

N. N. Nassar et al. (eds.), *Nanoparticles: An Emerging Technology for Oil Production and Processing Applications*, Lecture Notes in Nanoscale Science and Technology, https://doi.org/10.1007/978-3-319-12051-5_1

at least in one dimension, where unique phenomena enable novel applications [1]. Nanotechnology has emerged during the industrial revolution, although human exposure to nanoparticles has occurred throughout human history. The study of nanoparticles dates back to 1925, when the concept of nanometer was first proposed by Richard Zsigmondy, the 1925 Nobel Prize Laureate in chemistry. He explicitly used the term nanometer for the first time for characterizing particle size, and he was the first to measure the size of particles such as gold colloids using a microscope. Although he was the first in using the term, what we know now as "modern nanotechnology" was the brainchild of Richard Feynman, the 1965 Nobel Prize Laureate in physics. It was during the 1959 American Physical Society meeting at Caltech that he presented his well-known lecture, entitled as "There's Plenty of Room at the Bottom", in which he introduced the concept of matter manipulation at atomic levels.

This is from that time in history that our understanding of the modern nanotechnology has been born and developed over the decades. Now, we know him as the father of "modern nanotechnology". Norio Taniguchi, a Japanese scientist, was the first to use the term "nanotechnology" to describe semiconductor processes happening at nanoscale, almost 15 years after Feynman's memorable lecture at Caltech. The golden era of nanotechnology arrived in the 1980s when Smalley, Kroto and Curl discovered fullerenes and Eric Drexler of Massachusetts Institute of Technology (MIT) adopted ideas from Feynman's "There is Plenty of Room at the Bottom". Taniguchi's use of "nanotechnology" in his 1986 book entitled "Engines of Creation: The Coming Era of Nanotechnology" was one of the first definition of nanotechnology as "processing, separation, consolidation, and deformation of materials by one atom or one molecule". Afterward, Drexler suggested the idea of a "nano-assembler" which can build a copy of itself and of other items of arbitrary complexity, which later was known as "molecular nanotechnology". By developing carbon nanotubes by Iijima, another Japanese scientist, the science of nanotechnology was further advanced to a new level [2].

Nanoparticles have novel physical properties distinct from both molecular and solid-state matter due to their significant fraction of surface atoms. Study of these physical properties provides a unique way to learn how nanoparticles can be prepared and characterized. Knowledge of application of nanoparticles in different industrial settings dictates nanoparticles' preparation techniques and characterization. There are surface atoms in nanoparticles by which the nanoparticle "communicates" with its environment. Appropriate preparation techniques can lead to the formation of different types of nanoparticles which can be used as adsorbents and catalysts for different applications in energy and the environment. Different preparation techniques can result in different types of structures. These techniques, developed using appropriate experiments may give insights into complex issues in adsorption and catalysis, such as selectivity of binding of substrates to vertex, edge, or face sites on a nanoparticle. For example, nanosized metal, pharmaceutical, semiconductor, and simple or complex ceramic particles have numerous applications in the development of sensors, thermal barrier coatings, catalysts, pigments, drugs, etc. Considering diverse application, there are different techniques of nanoparticles'

preparations each associated with challenges. The challenges can range from controlling the particle size and size distribution to particle crystallinity, morphology, shape, being able to use the nanoparticles for a given application, and to produce them from a variety of precursors of choice. Different techniques of nanoparticles preparation are chosen according to being suitable for a range of applications and minimizing the challenges associated with such preparation methods. A general nanoparticle synthesis combines the advantages of low toxicity and cost of precursors and high yield of traditional aqueous-based colloidal chemistry with the size dispersion control. It was with this goal in mind that Boutonnet, Kizling, and Stenius first used aqueous pools of water in oil-continuous microemulsions to solubilize simple ionic metal salts of Au, Pd, Pt, and Rh, which was followed by chemical reduction using hydrazine or hydrogen gas to produce metal nanoparticles dispersed in oils [3]. Such novel nanomaterials are shown to have good catalytic activity for hydrogenation reactions.

Another industrially important nanoparticles can be categorized as polymeric nanoparticles (PNPs). Polymeric nanoparticles (PNPs) have gained considerable attention in numerous research activities and have been employed in encouraging number of domains during the last few years. They have been speculated as nanosized solid colloidal particles generated from polymers. Nanoparticles, which are originating from polymers, possess novel properties. PNPs' preparation techniques impose novel properties attached to them without the need for making new compounds. It is in their sizing that refashioning of their physicochemical characteristics happens, which is related to the magic which happens at nanoscale as is the subject in nanoscience and nanotechnology. The factors causing PNPs to attain relatively unique properties than bulk materials are connected to their reduced particle size. As already known, at nanoscale, quantum effects predominate, and the exposed surface area to volume ratio increases. Considering a crystal with many atoms, each atom will have different properties relative to those of bulk material. As seen in Fig. 1.1a, b, large surface area favors enhanced interaction with the surrounding material, specifically with the intermixed materials like composites as well as the performance of products like batteries, and reduces resource usage in catalytic processes, decreasing the amount of waste. This figure also demonstrates the transition effect from macro to nanoscale which causes the large surface area with reduced particle size (Fig. 1.1c) [4, 5]. Interaction of polymer confined to nanoscale with surrounding material makes them an ideal candidate for industrial application as high surface area is considerably a critical factor in the fabrication of new materials [6]. The PNPs' size and size distributions are remarkably interesting as they make for features such as surface area, packing density, viscosity, compact structure, and defined shape [7]. In this regard, Wang et al. [8] have developed variety of novel PNPs of different sizes and shapes using different preparation techniques.

PNPs' preparation techniques can differ to achieve different property optimization. PNPs can be prepared using two major categories named as chemical and physical preparation techniques. Chemical methods are used when monomer has been used as precursor, while physical techniques are implied when preformed polymers are used initially. If monomer is used as precursor, the PNPs' preparation

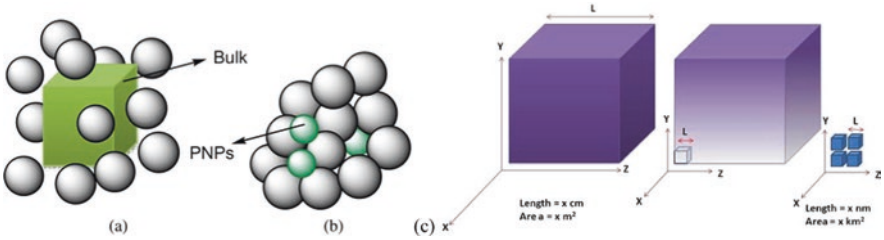

Fig. 1.1 Interaction with the surrounding (**a**) bulk polymer and (**b**) PNPs. (**c**). Large surface area with reduced particle size. Adapted from reference [4] after permission

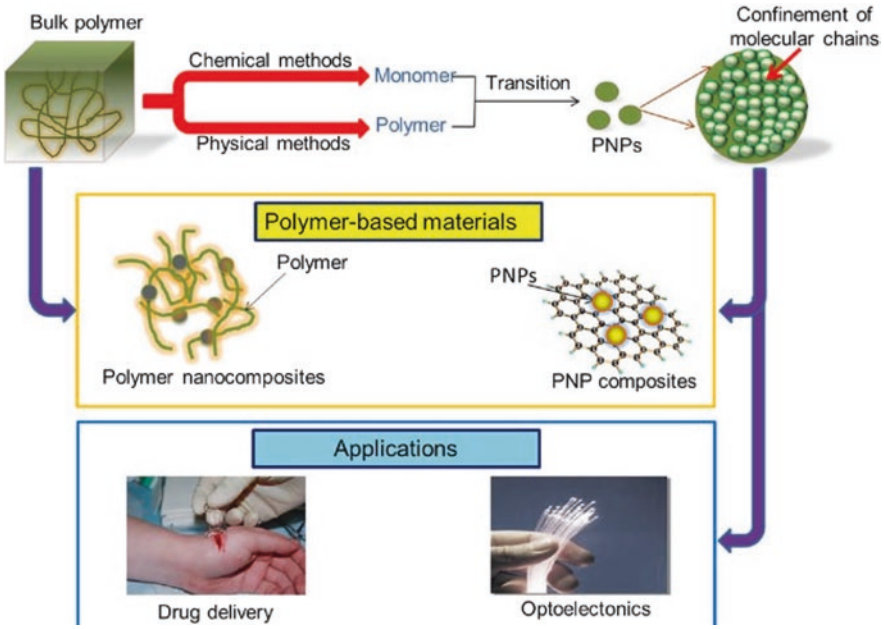

Fig. 1.2 From PNP's preparation to PNP's application. (Adapted from [4]) after permission)

techniques can be categorized as microemulsion, interfacial, conventional emulsions, mini emulsion, controlled radical, and surfactant-free emulsions. If a polymer is used as precursor, the nanoparticles' preparation techniques can be as diverse as freeze drying, solvent evaporation, salting out, spreading evaporation, nano-precipitation, dialysis, freeze extracting, fast evaporation, spray drying, etc. The diverse application of PNPs has been depicted in Fig. 1.2.

Several preparation techniques have been reported for nanoparticles manufacturing. This chapter is aimed at providing a summary of the two general techniques of nanoparticles' preparation, namely physical and chemical preparation techniques, and their characterization methods. These methods can be categorized into

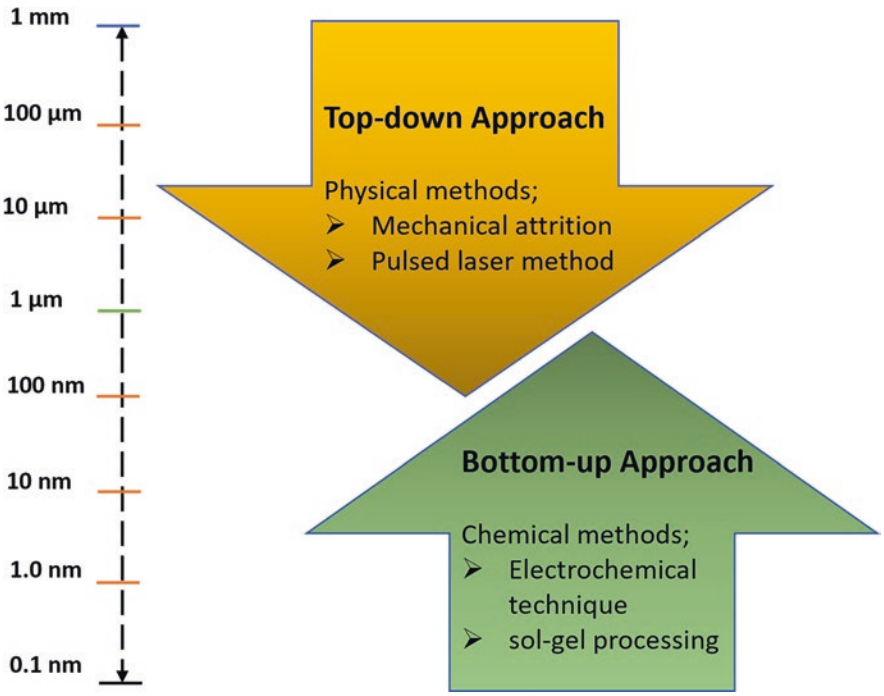

Fig. 1.3 Schematic representation illustrating the bottom-up and top-down approaches for nanoparticles preparation

bottom-up (chemical) and top-down (physical) techniques as shown in Fig. 1.3 [9]. The topics covered in this chapter include (1) the main bottom-up synthesis and top-down methods and its characterization; (2) importance of controlling nanoparticle size and shape; and (3) health and risk issue facing nanoparticles scaling up and applications at industrial level. The chapter also presents various factors and experimental conditions affecting the synthesis of nanomaterials in general.

1.2 Chemical Preparation Techniques

This preparation technique, also known as bottom-up, involves molecular components as starting materials linked with chemical reactions, nucleation, and growth processes to promote the formation of nanoparticles [10–14]. Six main techniques fall under the chemical preparation techniques category, namely: (1) chemical coprecipitation, (2) electrochemical, (3) sonochemical, (4) sol-gel processing, (5) chemical vapor deposition (CVD) and chemical vapor condensation (CVC), and (6) microemulsions.

Typically, in most of the aforementioned methods, a stabilizing agent is required during the synthesis to prevent aggregation of the resultant nanoparticles. A brief discussion on each technique with more focus on advantages and drawbacks, as well as suitability for field application is addressed.

1.2.1 Nanoparticle Synthesis by Chemical Coprecipitation

Coprecipitation is a well-established liquid phase synthesis approach that stands out for its ease of implementation at laboratory and industrial scale, rapid processing, low cost, and energy efficiency [15–17]. The precipitation/coprecipitation method requires the occurrence of supersaturation, nucleation, and growth steps, complemented by secondary steps such as aging (coarsening or Ostwald ripening) and/or agglomeration processes [17]. Figure 1.4 represents the overall steps of precipitation. Fundamentally, the coprecipitation method follows the principles of fast crystallization processes, although the former involves high initial supersaturation conditions and irreversibility or sparingly solubility of the products. The most prevalent and practical route to induce precipitation for nanoparticle synthesis is through chemical reactions, which are typically carried out by the rapid mixing of two concentrated solutions (>2000 rpm) [17, 18]. Addition/exchange, reduction, hydrolysis, and oxidation are the most distinguished of these chemical routes [19, 20]. Additionally, changes in temperature and fractionation of the solvent (through evaporation or crystallization) could also be used as approaches to induce supersaturation [17]. Such thermodynamic conditions promote fast nucleation and, thus, the successive growth of these resulting nuclei to form large numbers of visible crystallites. In parallel, these crystallites can either stabilize or coagulate/agglomerate in the solution [17, 19, 21]. In this final step, the coagulated nanoclusters can continue to grow until promoting sedimentation.

Although precipitation is a straightforward experimental technique feasible at moderate temperatures (<100 °C [16]), its thermodynamic and kinetic understanding is quite complex, especially in systems that involve tertiary and quaternary products given that multiple species precipitate simultaneously (hence, the term coprecipitation) [17, 19].

As shown in Fig. 1.4, nucleation is stated as the initial stage in coprecipitation. In general, this thermodynamic step involves the formation of a solid phase, hence requires overcoming an energy barrier for producing an interface between the bulk solution and the newly developed nuclei [20]. This barrier is determined by the total Gibbs free energy of the system (ΔG) and is driven by the supersaturation, temperature, and surface free energy conditions [20]. According to the fundamental theory, the nucleation ways that arise simultaneously in synthesis processes are classified into heterogeneous, homogeneous, and secondary nucleation. Heterogeneous nucleation is an inherent process that implies the presence of previous stable nucleating sites in the bulk solution [15]. According to Nielsen [21], the presence of solid impurities is a natural phenomenon, even in high-quality solvents, an average of 100

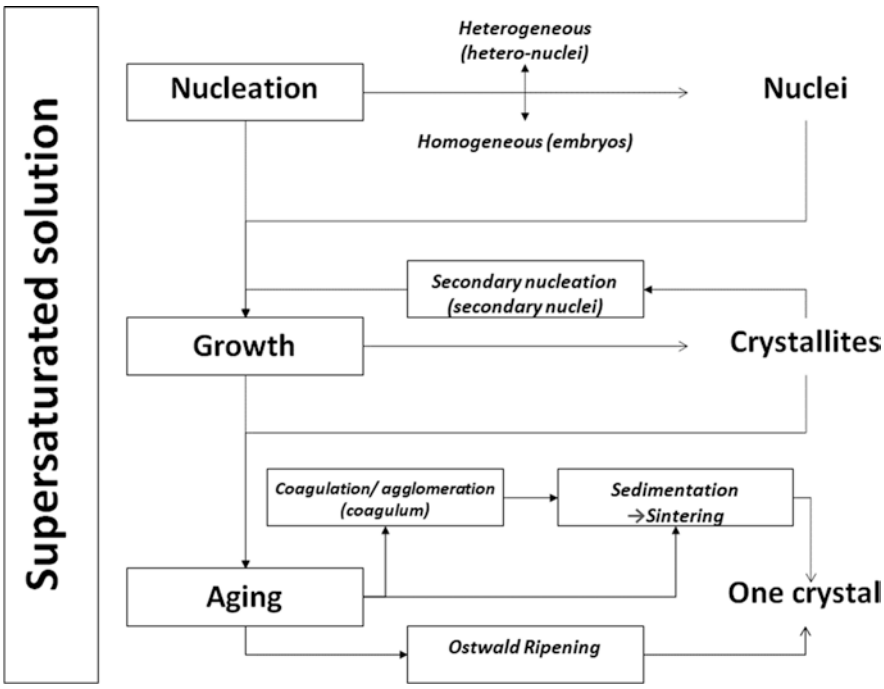

Fig. 1.4 Coprecipitation steps for nanoparticle synthesis. Idea adapted from reference [21] after some modifications

particles per mm^3 are present. These solid particles act as heteronuclei or catalysts for the initiation of precipitated crystals by the adsorption of elemental units that form a layer on the face of the crystal until it reaches sizes above the critical value, and thus, it can grow in the solution. The secondary nucleation is at some point analogous, since it refers to an intermediate state in the growth process from which the smallest crystallites serve as the "catalysts" for (secondary) nucleation. Meanwhile, in homogenous nucleation, there is a significant number of subcritical associates of crystal-like structure (embryos) in equilibrium with the bulk solution that spontaneously reach the critical size because of thermal fluctuations; these phenomena increase the probability of association above redissolution [19]. Therefore, this way of nucleation requires higher energetic barrier.

After the nuclei have been formed, they grow by the continued addition of new layers of elemental/molecular units (molecules, atoms, or ions) onto the surface of the nanocrystal. The transport phenomena involved are diffusion through the bulk solution (sometimes diffusion and convection combined) and one or more processes in the crystal solution interface (surface reactions) [19–21]. Therefore, the process can be either diffusion-limited or reaction limited, which depends on the precursor concentration; the limiting phenomenon is fundamental for the shape and size control of the nanoparticles. For instance, during the synthesis of monodisperse nanoparticles, diffusion-limited growth is the desirable process, although the final

shape of the nanoparticles will be closely linked to the surface reactions [19, 20]. Literature also recommends that for further increase monodispersity, capping ligands (surfactants or polymers) should be added to the system to promote steric repulsion between particles, as well as the induction of electrostatic repulsion by chemisorbed charged species (usually by changing the pH) [19]. Complementary, the secondary processes are also relevant in coprecipitation due to their fundamental contribution to thermodynamic stability. They involve minimization of the total surface free energy by reducing the interfacial area of the precipitates through processes known as aging. According to Nielsen [7], they include recrystallization of the primary particles to more compact shapes; the transformation of a crystal from a metastable modification into a stable modification by dissolution and reprecipitation; aggregation of primary particles followed by sintering (intergrowth); and Ostwald ripening, i.e., growth of the larger particles at the expense of the smaller ones.

Based on the above, this technique, from the experimental point of view, poses important theoretical challenges. Control of morphology, size, and dispersibility of the nanoparticles are linked to the interplay of nucleation and aggregation processes. Some authors have grouped the most relevant experimental parameters that play fundamental roles in controlling the thermodynamic and kinetics of these steps [15, 19, 20, 22], besides the concentration of precursors and temperature; pH and ionic strength, nature of the solvent, heteronuclei/seeds and templates, and capping ligands are recommended to be included and/or modified during the synthesis. To illustrate, the solubility product constant, Ksp, which is a very useful parameter for calculating the solubility of sparingly soluble compounds, tends to be very low in hydroxides, carbonates, phosphates, oxalates, and chalcogenides, which make them suitable precipitants [18, 19, 23]. Furthermore, remarkable experimental works, such as the presented by Jia et al. [24], showed the effect of pH on the growth rate of α-Fe_2O_3. At pH ≥ 6, 2D snowflake-like α-Fe_2O_3 dendrites were formed; while at pH ≤ 5, 3D houseleek-like α-Fe_2O_3 NPs were generated. Several other reports have focused on the capping ligands, such as polymers (which are the most popular ligands) like polyvinylpyrrolidone (povidone, PVP) [25–27], polyacrylic acid (PAA) [28], polyetherimide (PEI) [29], polyvinyl alcohol (PVA) [30, 31], and poly(ethylene glycol) (PEG) [32], and surfactants such as cetyltrimethylammonium bromide (CTAB) [26, 33, 34] and sodium dodecyl sulfate (SDS) [35], among others.

1.2.2 Nanoparticle Synthesis by Electrochemical Methods

Electrochemical deposition or electrodeposition methods have been categorized as a potential alternative, environmentally friendly/low emission (since electrons are used as a reagent, the use of hazardous reagents can be avoided [36]), easily controlled (by switching on/off the power supply [36]), and economical competitive technique for the synthesis of a wide variety of nanostructured materials, including semiconductors, superconductors, electrically conductive polymers, and biomaterials, for different kind of industrial applications such as catalysis, sensing and

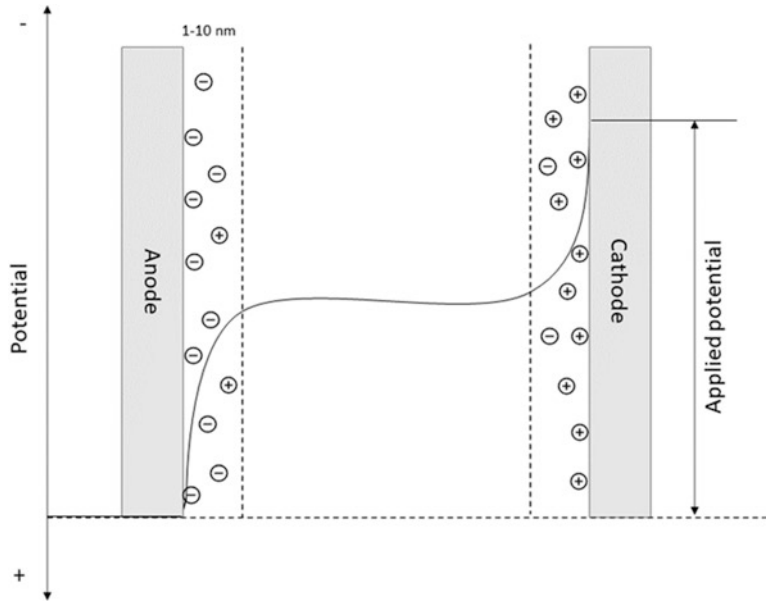

Fig. 1.5 Electrical double-layer model [36]

biosensing, medicine, optics, environmental remediation, nanorobotics, and microelectronics, among others [37–40]. In general, electrodeposition consists of the formation of solid or condensed matter deposits on conducting surfaces through electrochemical reactions that are driven by an external source of current or voltage [37, 38, 41]. A basic explanation of electrodeposition arises by the fundamental understanding of the simple two-electrode electrolytic electrochemical cell, as shown in Fig. 1.5. When the electrodes submerged in an electrolyte solution (usually aqueous-based formed from either simple salts or complexes) are polarized, it implies the appearance of a charge imbalance across the electrode–electrolyte interface that is neutralized by the migration of the nearest charged species (electrons or ions [42]) in the solution to the electrode surface within a few hundredths of a second. The interaction between the adsorbed species and the electrode surface promotes the appearance and growth of an electrical double layer (Fig. 1.5). The induced potential gradient is no longer represented by the gradient observed in the bulk solution (which is in the order of 1 or more volts), it is gathered in the thickness of the double layer, which implies an extremely steep gradient (~106 V/cm) and, thus, a high-intensity electrical field [36] (see the potential curve in Fig. 1.5). Therefore, the electromotive force supplied by an external source in this method represents the driving force, as mentioned before. In this regard, increases in the polarization intensify the electron transfer reaction at the electrodes and the consequent phenomena of charge imbalance/neutralization (a continued Faradaic current is observed) [36].

On the other hand, as the potential drop across the working electrode–electrolyte interface must be controlled, it is practical to consider the conventional three-electrode system in which the functions of the counter electrode are divided between a reference electrode (with negligible polarization, being the most popular, the standard hydrogen electrode (SHE), saturated calomel electrode, or mercury chloride (SCE), and silver/silver chloride (Ag/AgCl) [43]) and an auxiliary electrode (that carries the current, such as carbon or graphite, platinum, gold, lead, and titanium [36, 43].). Thus, the potential is controlled between the reference and working electrodes, while the current passes between the auxiliary and working electrodes [36]. The auxiliary electrode usually has a bigger surface area in comparison with the working electrode, to guarantee that the half-reaction occurring at its surface occurs faster, avoiding limitations of the process at the working electrode.

Against this background, the electrodeposition can be controlled by either an applied potential or current, being classified as potentiostatic and galvanostatic, respectively [36–38]. The control of the potential/current input allows that the reacting species overcome an energy barrier (activation energy) to make thermodynamically feasible the reduction/oxidation couple. In that sense, the spotlights are the energy of the electrons of the working electrode and those of the electroactive species. In the former, the Fermi-level (E_F), which refers to the energy of the highest occupied orbitals (HOMO) in metals, can be controlled by the external potential (when a negative potential is applied, E_F moves to higher energy; when a positive potential is applied, E_F moves to lower energy [36]) until it reaches a lower level than the HOMO of the active molecules in solution, allowing the electron-transfer processes to the electrode. The critical potential at which this electron-transfer process occurs is known as the standard/equilibrium potential (E_0) of the reduction/oxidation couple. Therefore, the difference between the applied positive potential (E_i) and E_0 is known as overpotential (OPD) [36].

Once the current density is increased in the cell or the OPD condition is reached, the adsorption of the active species on the surface of the substrate is promoted until the final development of nanostructures. The overall process is analogous to that explained in coprecipitation, i.e., it comprises the fundamental steps of nucleation and growth, which are grouped in two major processes, deposition and electrocrystallization [38]. Figure 1.6 is a schematic representation of the overall electrodeposition process. In brief, the initial step is the mass transportation (immigration, diffusion, and convection) of solvated ions (in aqueous electrolytes, hydrated ions) from the bulk toward the cathode. At the border of the electrical double-layer OHP occurs the charge-transfer reaction, i.e., the ions partially desolvate/dehydrate until their attachment onto the substrate cathode surface. Finally, the ad-ions and the consequent ad-atoms are formed. Surface diffusional phenomena appear until the completed lattice incorporation of the ad-atoms that results in nucleation of stable atomic clusters and, eventually, their growth [38]. In parallel, depending on the magnitude of the difference between the applied and standard potentials (E_i and E_o), the kinetics of the process can be activation (charge transfer) controlled, mixed controlled, or diffusion controlled. Initially, electron transfer rates are dramatically increased, and the potential–current density (voltammetric curve) grows

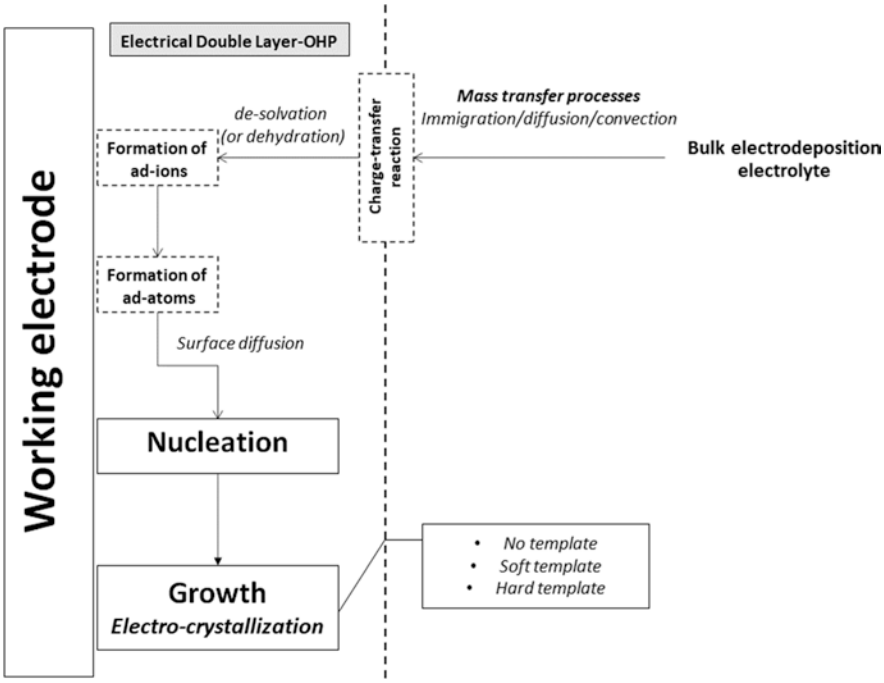

Fig. 1.6 Electrodeposition steps for nanoparticle synthesis [38]

exponentially (Butler–Volmer model); then, the voltammetric curve reaches the mixed region in which the diffusion and activation rates both limit the electrolysis current. Finally, the currents are purely diffusion limited, and peak or plateau currents are observed in quiet and stirred solutions, respectively [36, 38].

Analogously, several experimental parameters can be modified/applied for controlling the thermodynamic and kinetics of the process, besides the input potential/current; the following factors should be considered: nature of the substrate (crystal structure, specific free surface energy, and lattice orientation, among other); type of electrolyte (aqueous or ionic); pH; the use of templates; agitation; stabilizing agents; area of the electrodes; and time of exposition; among others. To illustrate, the synthesis of shape-controlled nanostructures (mainly nanowires and nanorods) is significantly improved when soft and hard templates are used. Among the most popular soft templates are surfactants and polymers [44–48]; as well as microemulsions [37, 49, 50]. Likewise, the most common and available hard templates are anodized alumina (AAM), as wells as inorganic and polymeric membranes [40, 51, 52]. Furthermore, potentiodynamic or pulsed electrodeposition is also used, mainly to improve the control in the growth step, allowing the system to experience periods in which electrodeposition occurs and others in which the nearest electroactive species recover [37].

1.2.3 Nanoparticle Synthesis by Sonochemical Methods

In the direction of reaching important technological developments at the nanoscale that, at the same time, are in synchrony with ecofriendly chemical synthesis processes, the use of alternative energy sources, such as electromagnetic and mechanical waves, has been widely contemplated for the activation of chemical reactions in recent years, avoiding excessive consumption of hazardous reagents and generation of waste [53]. Among these techniques, sonochemistry is one of the most relevant due to its superiority at certain fundamental aspects in comparison to all other nanoparticle synthesis techniques. Gedanken [54] highlighted the advantages of sonochemistry in the following areas: preparation of amorphous products, insertion of nanomaterials into mesoporous matrices, deposition of nanoparticles on ceramic and polymeric surfaces, and formation of proteinaceous micro- and nanospheres. Other positive aspects of sonochemistry are the short time of reaction, high purity of products, and narrow size distribution with large surface area of the nanoparticles [53, 55].

The fundamentals of sonochemistry arise from the application of powerful ultrasound radiation (20 kHz–15 MHz [54, 56–58]) to stimulate chemical reactions in a liquid solution. These chemical effects proceed from nonlinear acoustic phenomena, primarily acoustic cavitation, i.e., formation, growth, and implosive collapse of bubbles [57, 58]. As a result of the collapsing phenomena that occur in less than a nanosecond, a huge amount of energy is released into the liquid; therefore, local heating, high pressures, and high-speed jets (with speeds >100 m/s [55, 56]) are produced. Such localized hot spots that reach very high temperature (5000–25,000 K [58]), pressure (>100 MPa [54, 57, 58]), and high cooling rates (1011 K/s [54, 57]) are responsible for the appearance of turbulence in the flow of the liquid and an improved mass transfer, causing the thermomechanical conditions capable of cleaving the intermolecular bonds of the precursors [53]. Likewise, the mechanisms of product generation depend on the quality of the reagents (mainly volatility) and the conditions of the reaction, which classifies the sonochemistry as primary (gas phase chemistry occurring inside collapsing bubbles) and secondary (solution phase chemistry occurring outside the bubbles) [55, 57, 59]. In the former case, a volatile precursor produces free metal atoms generated by bond dissociation (e.g., metal–carbon bonds in organometallic compounds [60]) due to the intense thermodynamic conditions reached during bubble collapse; these newly formed atoms nucleate to form nanostructured materials [57]. Additionally, because of high cooling rates, the organization and crystallization of the products are inhibited and, thus, amorphous nanoparticles are developed [54, 59]. In the case of nonvolatile precursors, the sonochemical reactions occur in the solvent phase. After the bubble collapse, the surrounding liquid also experiences transient heating within a ring region of 200 nm, reaching temperatures above 1900 °C [54, 56, 59]. The resultant high-energy species (e.g., radicals) diffuse into the liquid phase and react, leading to the formation of nanoparticles [57]. In this case, the products are sometimes amorphous nanomaterials or, in other cases, nanocrystalline. The final structural organization will depend on the temperature of the ring region [54].

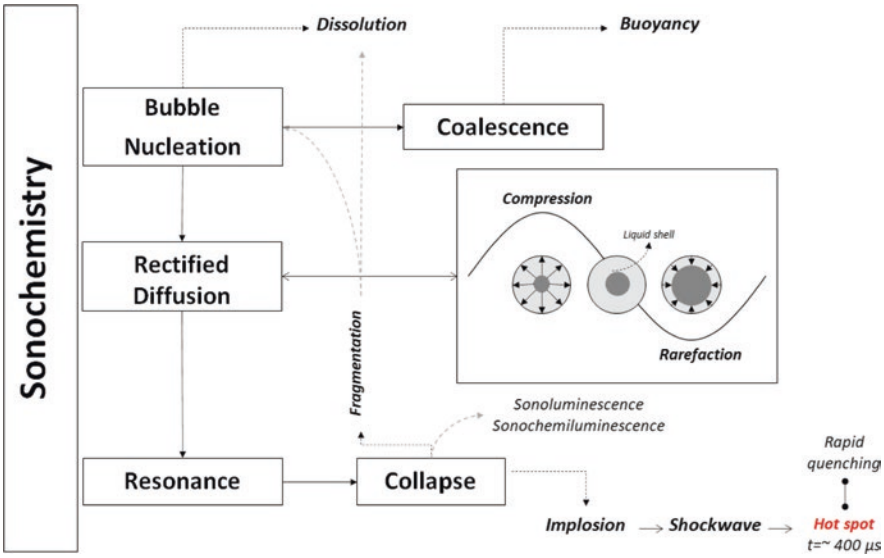

Fig. 1.7 Sonochemistry steps for nanoparticle synthesis. Part of figure is adapted from reference [61] with permission

From a fundamental point of view, acoustic cavitation stimulates several complex processes in the generated bubbles; thus, a theoretical understanding of these phenomena can lead to enhanced control of the method. Figure 1.7 summarizes schematically the distinct stages that the bubbles can go through. In general, the initiation step corresponds to the bubble nucleation that arises because of preexisting impurities in the solvent phase (small gas bubbles protected by a skin of organic impurities, bubbles trapped in motes or crevices in solid surfaces [57, 61]). Sequentially, when the applied acoustic pressure is above a certain threshold, the growth step begins. The pathways of this step are coalescence and, mainly, rectified diffusion [61]; this latter process is fundamental for describing the interlink between growing and mass diffusion across the air–liquid interface: as the acoustic cycle alternates between the compression and rarefaction (see Fig. 1.4), gas is forced to diffuse in and out of the bubbles [56]. The changing area and liquid shell are considered the two main contributors to rectified diffusion; when the bubbles shrink, the surrounding gas will be concentrated near the interface (Henry's Law), and the liquid shell will become thicker, reducing the driving force for the diffusion of gas out of the bubble. By contrast, the expansion of the bubbles will reduce the liquid shell; thus, the driving force for the inlet diffusion will increase [56, 61]. Therefore, the area and shell effects synergistically contribute to a net mass diffusion into the bubble over time or growth ($t < 100$ µs, bubble ratio < 50 µm) that finishes with an adiabatic implosive collapse, and the subsequent formation of nanostructures. According to Gedanken [54], these nanostructured products are the consequence of the fast kinetics that inhibit the nuclei growth. Because of the described physicochemical effects, several experimental parameters can be modified/controlled

during the overall process to improve the quality of the nanoproducts, including acoustic power, frequency, hydrostatic pressure, properties of the solvents and reagents (mainly boiling temperature and ratio), the inclusion of templates and their nature, process temperature, and sonication time, among others [53]. To illustrate, in the synthesis of nanostructured noble metals, the use of nonvolatile precursors dissolved in volatile solvents such as water is a common practice, considering that sonolysis of the water vapor produces chemical intermediates (specifically H radicals and $e(aq)^-$) that act as strong reducers species in redox reactions. Thus, chemical-reducing agents can be avoided, although alcohols (e.g., 2-propanol, ethanol [62]) and surfactants (e.g., SDBS, SDS, PVP, PEG, CTAB [62]) are also recommended to generate secondary radicals, which can dramatically promote the reduction rate [67, 71]. On the other hand, the use of volatile organometallic precursors (e.g., $Fe(CO)_5$, $Ni(CO)_4$, $Co(CO)_3NO$, $Mo(CO)_6$, $W(CO)_6$ [57, 60]) dissolved in nonvolatile solvents (e.g., silicone oil, polyethylene glycol, ethylene glycol [57, 62, 63]) has the particular advantage of achieving more secure conditions, due to the capacity of the solvents of absorbing the energy (via rotational and vibrational molecular modes, ionization, and competing bond dissociation [57]).

1.2.4 Nanoparticle Synthesis by Sol-Gel Processing

Sol-gel processing is a well-documented and cost-competitive wet chemical method that stands out for its low-temperature reaction, good composition control (high purity products and stoichiometry level), production of shaped and homogeneous nanomaterials (e.g., bulk monoliths, fibers, powders, sheets, coatings, films), large-scale industrial production, and broad applicability, mainly in material science and ceramic engineering [64–67]. From a general perspective, the sol-gel method involves the preparation and subsequent transformation of a sol (which refers to a dispersion of colloidal particles in a liquid medium with diameters between 1 and 100 nm [68]) into a gel-like intermediate (an oxide or alcohol-bridged network) because of the simultaneous hydrolysis and polycondensation of a precursor (either inorganic metal salt or metal–organic) that promote dramatic increases in the viscosity of the dispersion (syneresis) until the final transformation into a functional solid nanomaterial; complementary processes such as thermal treatment are essential for the remotion of the solvent from the interconnected gel network (drying) and the calcination of this gel (dehydration) [19, 68]. Due to the resultant drying stress, monolithic gel bodies are often destroyed, and powders are obtained [69]. Figure 1.8 represents the overall steps of sol-gel processing.

In principle, the precursors, either alkoxide or solvated metals, are dispersed into an aqueous solution to induce hydrolysis and simultaneous (competitive/complementary) condensation reactions. However, it is important to highlight that the reaction routes differ substantially as a function of the precursors; therefore, a specific description of the processing in virtue of their nature is fundamental and discussed below.

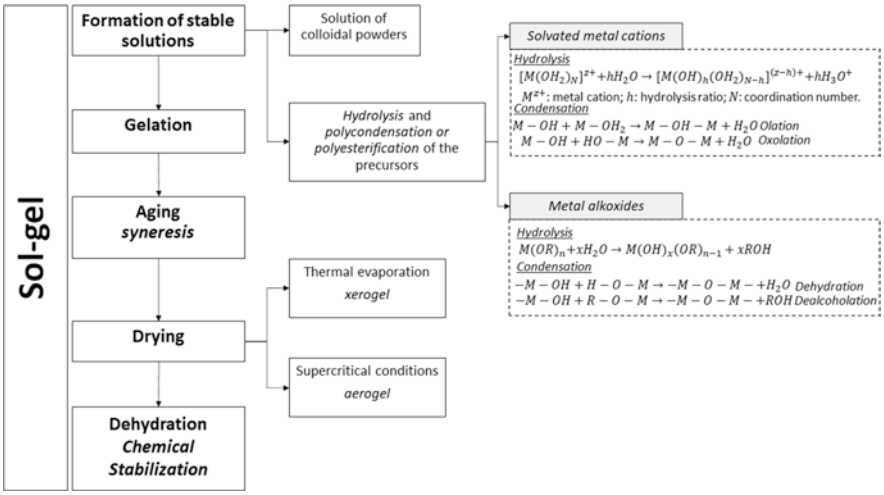

Fig. 1.8 Sol gel method's steps for nanoparticle synthesis [19, 65, 70, 73]

Solvated Metal Cations In an aqueous medium, metal cations (M^{z+}) are solvated by dipolar water molecules, giving rise to aquo ions ($[M(OH_2)_N]^{z+}$). This electron transfer process occurs from the bonding orbitals of coordinated water molecules toward empty orbitals of the metal cation, $M^{z+} + NH_2O \rightarrow [M(OH_2)_N]^{z+}$, where N is the coordination number of the cation [70]. Likewise, the transfer process also results in weakening the O–H interactions of bounded water that becomes more acidic. The resultant hydrolysis (deprotonation) reaction is as follows:

$[M(OH_2)_N]^{z+} + hH_2O \rightarrow [M(OH)_h(OH_2)_{N-h}]^{(z-h)+} + hH_3O^+$, where h is the hydrolysis ratio.

In dilute solutions, the reaction can produce monomeric species ranging from aquo cations ($[M(OH_2)_N]^{z+}$), hydroxy species ($[M(OH)_z]^0$), and oxo anions ($[MO_m]^{(2m-z)-}$), when all the protons have been removed from the coordination sphere of the metal cation [70]. These equilibria depend mainly on the pH, and, in a lesser extent, temperature and concentration. The theoretically analysis of this reaction is generally based on the electronegativity equalization principle or Partial Charge Model (PCM) [19, 70]. Thus, the proton exchange between the precursor ($[M(OH)_h(OH_2)_{N-h}]^{(z-h)+}$) of mean electronegativity χ_h and the aqueous solution of mean electronegativity χ_w proceeds until they reach equal values ($\chi_h = \chi_w$) Parallelly, χ_h depends on the metal cation (M^{z+}) and the hydrolysis ratio (h) at a given pH. The charge-pH diagram (refer to [19, 69, 70]) is a useful guide because it is possible to predict the parameters that favor condensation reactions, as they are only possible when the system is brought from the aquo (low-valent cations) or oxo (high-valent cations) domains to the hydroxy domain, i.e., OH groups must be present in the precursor [19, 70]. Based on the above, the condensation reactions are promoted mainly by pH variations. According to Henry et al. [70], condensation is initiated by adding a base to low-valent metal ions (e.g., Cu^{2+}, Al^{3+}, Zr^{4+}) or an acid to

high-valent metal ions (e.g., W^{6+}, V^{5+}). Redox reactions are also initiators [70]. Furthermore, the condensation of hydrolyzed metal ions follows two main mechanisms: *olation* when $N = z$, i.e., nucleophilic attack (substitution) of a negatively charged OH group ($[\delta(OH^-)]$) to a positively charged metal cation ($[\delta(OH_2)]$), that produces "*ol*" bridges ($M-OH-M$, see the reactions in Fig. 1.8); and *oxolation* when $N - z > 0$, i.e., nucleophilic addition of OH groups onto metal ions, followed by the formation of an "*oxo*" bridge ($M-O-M$, see the reactions in Fig. 1.5) [70].

Metal Alkoxides In this case, hydrolysis is induced because of the introduction of water or water alcohol mixture into the system. The reaction is initiated through nucleophilic attack (substitution) of H_2O molecule to a positively charged metal atom, generating the insertion of hydroxide groups into the coordination sphere of the metal atom ($[M(OH)_x(OR)_{n-1}]$). Analogously, the rate of substitution depends on the coordination instauration of the metal atom ($N - z$); higher values of ($N - z$) require lower activation energy of the nucleophilic attack [71]. Equally important, the alkoxide/water ratio $\left(\frac{M(OR)_n}{H_2O} = x\right)$ determines the number of substituted alkoxy groups. Thus, variation and control of x has profound consequences in the morphology and structure of the resulting gel [19]. Simultaneously, after the insertion of hydroxide groups, condensation occurs in the following ways [65]: *dehydration* or *dealcoholation* (see the reactions in Fig. 1.8).

The second step of the overall process is gelation, which appears because of the hydrolysis and polycondensation reactions by the random collision of polymeric species in solution, leading to crosslinking bridges (oxide or alcohol) that eventually become a three-dimensional network [65]. As already mentioned, the main characteristic of this step is the sharp increase of the viscosity. Casting is also common to stimulate the formation of specific shapes, which can be easily recovered at the end of the process, by just ejecting the product out of the mold. Complementary, this developed network is further subjected to polycondensation for a period of time (hours to days), leading to decreases in the porosity of the interconnected system in a process known as aging (syneresis); thus, the aged gel must reach high strength to avoid any cracking during drying. In this last process, the solvent is removed from the crosslinked network by either thermal evaporation (xerogel) or supercritical solvent extraction (aerogel) [68, 72]. In the former case, large capillary stresses appear (in small pores <20 nm [68]) due to increases in the coordination numbers of the particles that result in the formation of additional linkages and the consequential collapse of the network; therefore, considerable shrinkage and reduction in the surface area and pore volume are the main consequences observed in thermal evaporation [19, 72]. A practical solution is the use of surfactants that decrease the surface energy of the solvent or supercritical extraction (capillary stresses disappear due to the lack of solvent–vapor interfaces [19]). The most common method is removing the pore fluid above its critical point, although an alternative route is replacing the solvent with CO2 and then removing it above its critical point [72]. As discussed, aerogels are low-density materials with high surface area (200–1000 m^2/g [73]) and controlled pore size distribution. Finally, the gel is dehydrated to desorb the

hydroxyls, avoiding rehydration processes. To get this stabilized gel, the sample is calcinated at a temperature in the range of 500–800 °C [19, 68].

Analogously to the other methods, there are critical experimental parameters that can be controlled to increase the efficiency of the process. Particularly, in this method, these aspects are well differentiated: pH of the solution (acid- or base-catalyzed hydrolysis of metal alkoxides [74–77]), the molar ratio of water to alkoxide [78], and temperature [79].

1.2.5 Nanoparticle Synthesis by Chemical Vapor Deposition (CVD) and Chemical Vapor Condensation (CVC)

Chemical vapor deposition (CVD) and chemical vapor condensation (CVC) are distinctive material processing techniques that are characterized for their capability of producing highly dense and pure materials, as wells as nanoparticles with narrow size and homogeneous films with good reproducibility and adhesion as they can coat complex-shaped substrates uniformly [80]. Their fields of applicability include electronics, optoelectronics, surface modification, and biomedicine [81]. In these methods, vapor phase precursors are convectively transported into a high-temperature reaction chamber to promote thermal dissociation and/or chemical reactions on or near the vicinity of a substrate to form stable solid products [80–82]. In this regard, when the nucleation step is favored in the vapor phase and ultrafine clusters or nanoparticles are formed, the approach is defined as vapor synthesis or CVC (thus, it requires activation energy to proceed) [83, 84]. Analogously, when the nucleation step is favored onto the surface of a heated substrate (which acts as the activation energy source), deposition and adsorption of the active gas species and reaction intermediates are stimulated, and the method is differentiated as CVD [80–82]. Regardless of these variations, which are mostly associated to the hierarchy of the experimental systems and equipment, the physicochemical principles of both methods are equivalent. According to Choy [80], the chemical reactions that proceed can be classified as: thermal decomposition (pyrolysis), oxidation, reduction, hydrolysis, nitridation, deprotonation, photolysis, and/or combined reactions.

On the one hand, the CVC setup mainly consists of a feed system and a reaction chamber that is maintained under vacuum. The injected precursors flow through a tubular reactor where gas-phase homogeneous reactions take place within a short residence time (<0.1 s), driving to the fundamental steps of nucleation and growth. At the outlet, the two-phase stream (gas and nanostructures) is subjected to a rapid expansion that serves to mitigate undesired agglomeration processes. Finally, the nanoparticles are deposited on a rotating nitrogen-cooled substrate. Figure 1.6 represents schematically the steps of CVC [83, 84]. A relevant aspect of this technique is its linkage with some Physical Vapor Deposition (PVD) methods; according to Chang et al. [83], this technique takes the advantages of the significant energy provided by laser beam, combustion flame, and plasma in the thermal decomposition of

organometallic precursors, as well as the Inert Gas Condensation (IGC) synthesis methods, that lead to the evaporation and condensation of volatile species in a reduced pressure environment. Therefore, CVC is useful in processing almost all kind of precursors. The main experimental aspects that must be rigorously controlled were summarized by Tavakoli et al. [84] and involved low concentration of precursor in the carrier gas to minimize the collision frequency of the formed nanoclusters, expansion of the ejecting gas stream, and rapid quenching of the gas-phase nucleated clusters.

On the other hand, as CVD is more thermodynamically feasible (e.g., it does not require high vacuum working environments), scientific literature has extensively focused on this method [85–87]. The overall processes involved are summarized in Fig. 1.9. First, the reactant gases are transported into the chamber to induce, either gas-phase homogenous reactions that generate byproducts and intermediates, or the eventual diffusion of these gaseous precursors to the boundary layer of the substrate. Both the precursors and intermediates adsorb onto the substrate surface; and phenomena such as heterogeneous chemical reactions and surface diffusion are promoted, which contribute to the induction of nucleation and the subsequent growth steps. Alongside, some byproducts and unreacted species desorb from the surface and are directed to the effluent gas treatment system [80–82]. According to Choy [80], the most relevant experimental parameters to control in the process are deposition temperature, pressure, input gas ratio, and flow rate, the temperature being the dominant parameter. This deposition rate–temperature correlation generally fitted an Arrhenius model, i.e., high surface temperatures increase thermally activated reactions, which induce higher deposition rates and thus enhanced surface diffusion processes of the atomic species and growth rates. This region is defined as the

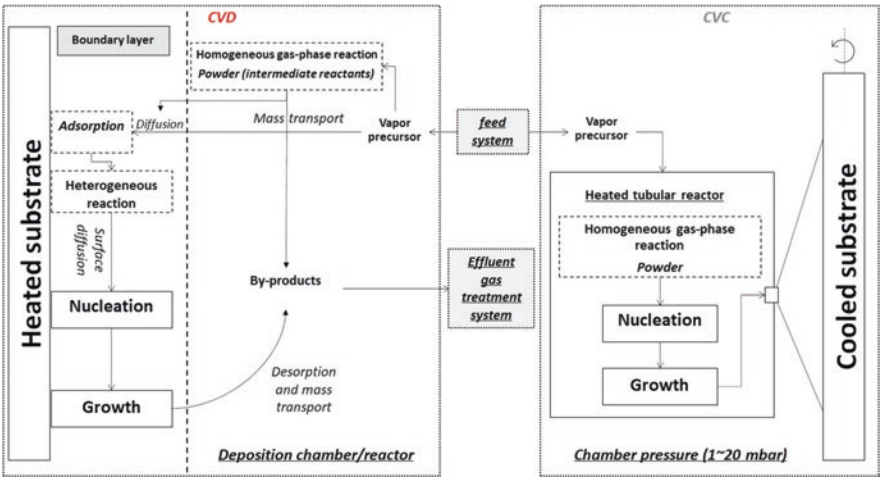

Fig. 1.9 Chemical Vapor Deposition (CVD) and Chemical Vapor Condensation (CVC) steps for nanoparticle synthesis [80, 81, 83]

chemical kinetics limited zone [80, 82]. The main characteristic is the homogeneity of the formed films that is reached by controlling the temperature over the substrate surface. Nevertheless, if the temperature further increases, the growth rate becomes almost independent, and the process is controlled by the mass transport of the precursors through the boundary layer, and this region is known as mass transport limited [80, 82]. Besides the operation temperature, pressure is also considered a relevant parameter in this method. Although CVD processes are viable at atmospheric pressures, some subdivisions have been stipulated regarding the working pressure ranges as atmospheric-pressure CVD (APCVD) or low-pressure CVD (LPCVD, ~0.1 10 torr). The particularity of the LPCVD condition is that the process is mass transport limited [80]. Furthermore, there have been developed some advanced technological variants of CVD systems, mainly focused on the type of energy sources, such as plasma enhanced CVD [88–90], photo-assisted CVD [91], and laser-assisted CVD [92, 93].

1.2.6 Nanoparticle Synthesis by Microemulsions

Microemulsion-based (ME) synthesis is a low-temperature powerful method for the preparation of high-quality colloidal nanoparticles, characterized by comprising low-cost instrumentation and good control of stoichiometry, size, homogeneity, and morphology of the products due to its ability to mix reactants efficiently at the molecular level [94, 95]. It is widely used in sensing, catalysis, and biomedicine for drug-delivery systems involving mainly polymeric nanoparticles [96]. Essentially, this approach embraces surfactant-stabilized droplets phase that acts as the "nanoreactors" (diameters varying between 2 and 50 nm [96, 97]), leading to flexibility, accessibility, and adaptability of the precursors and reactions. Therefore, nanoparticles can be synthesized in water-in-oil (w/o), oil-in-water (o/w), and/or bicontinuous microemulsions, i.e., polar/hydrophilic- (w/o-ME) or nonpolar/hydrophobic- (o/w-ME [97]) droplets/nanoreactors. The complete microemulsions schemes in virtue of the dispersed phase (w/o-ME or o/w-ME) are schematically represented in Fig. 1.10. In general, the synthesis of nanoparticles in o/w-MEs has the advantages of low environmental impact (since the continuous phase is water) and stable phase behavior (interactions between the organometallic precursors and surfactants are weaker) [97]; while the w/o-MEs have been categorized as the most important and widely implemented technique because of their easy formulation and affinity with the abundant water-soluble metallic salt precursors [94].

According to Sanchez-Dominguez et al. [97], two strategies have been identified for the synthesis of inorganic nanoparticles in o/w-MEs: oil–water interface controlled microemulsions, in which the precursor is an ionic salt dissolved in the water continuous phase; and single microemulsion, in which the precursor is an organometallic salt dissolved in the oil droplets of the microemulsion (see the detailed schemes in Fig. 1.10). In the former, the precipitant agent and the metallic precursor (A and B) dissolved in the continuous phase are transferred and adsorbed on the

oil–water interface. Initially, the diffusion of the metallic cations is driven by the electrostatic attraction with the anionic part of the surfactant to increase the stability of the system. After a while, the precipitant agent is added and the balance is destroyed, which leads to the occurrence of the reaction at the interface and the subsequent fundamental nucleation and growth steps that proceed until the final formed nanostructures [97, 98]. The two pathways of these steps are intramicellar and/or intermicellar nucleation and growth. For the first one, the reactions are located close to a droplet interface, and electrically neutral nanoclusters are formed. Eventually, the surfactant encapsulates them, as they are unstable at the interface, and promotes phase-transfer processes. On the other hand, reactions can also occur at the shared interfaces of two collapsing micelles, and the process is termed as

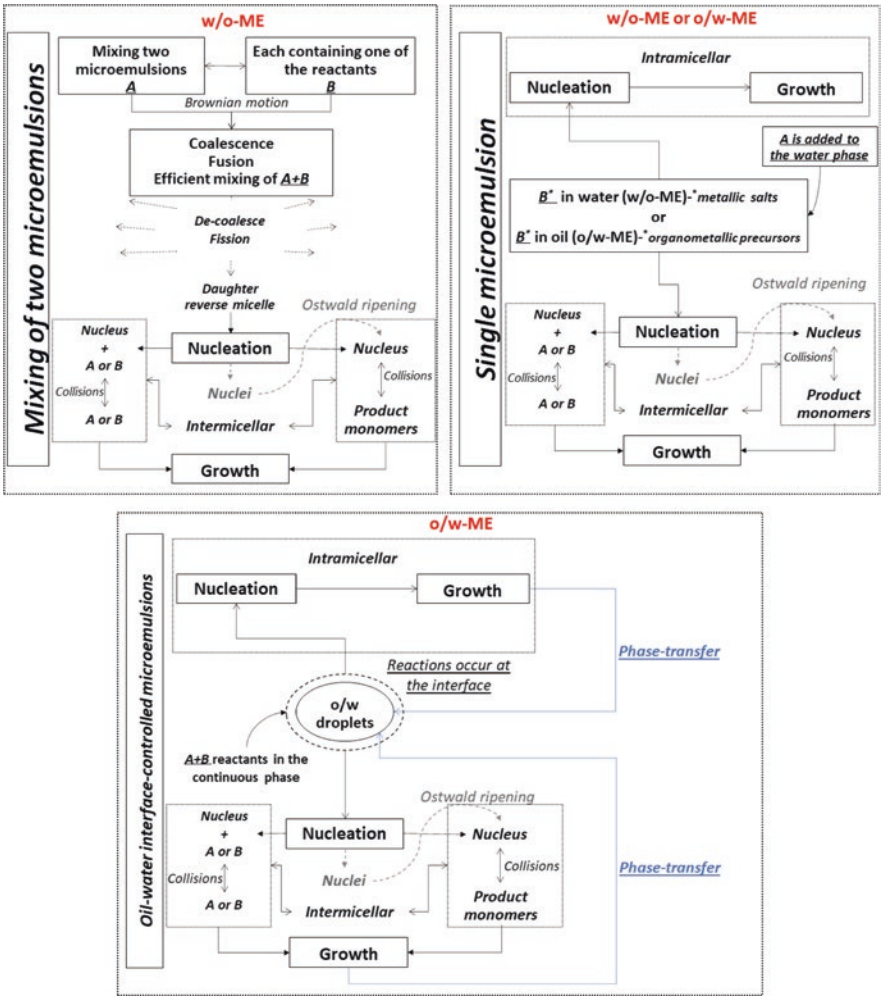

Fig. 1.10 W/O and O/W microemulsion schemes for nanoparticle synthesis [94, 97]

intermicellar [97, 98]. The consequent steps are analogous to the explained above, as they involve phase transfer of the hydrophobic nanoparticles. In both cases, the hydrophobic nanoparticles can be precipitated, or the system can be subjected to hydrothermal treatment for increasing crystallinity [97]. Furthermore, the single microemulsion synthesis route is a straightforward approach, considering that the organometallic precursors are dispersed in the oil droplets of the o/w-ME; thus, the only action required is the incorporation of the precipitating agent (typically water soluble) at a delayed time to promote intramicellar and/or intermicellar nucleation and growth steps.

In a similar way, Husein and Nassar [94] identified two strategies for the synthesis of nanoparticles in w/o-MEs: mixing of two microemulsions, in which each of the mixed w/o microemulsions contains one of the reactants; and single microemulsion, in which the precursor is dissolved in the water droplets (see the detailed schemes in Fig. 1.10). In the former, intermicellar nucleation and growth is the synthesis route, because of fusion and subsequent fission processes of micelles that are driven by Brownian motions. Initially, the collisions promote coalescence, fusion, and efficient mixing of reactants. Sequentially, the chemical reactions proceed at their intrinsic rate of reaction; for instance, in fast reaction scenario, the rate is controlled by the collisions between reverse micelles (which in turn is governed by the rigidity of the surfactant layer); in contrast, for slow reactions, the rate depends on the statistical distribution of the reaction species among the reverse micelles (they are typically well described by Pseudo continuous models). The final step is decoalesce/fission into daughter reverse micelles where the reactions occur, and the following nucleation and growth steps. The possibilities of growing scenarios are represented in Fig. 1.10, e.g., a micelle carrying a nucleus collapse with another one carrying product monomers. Furthermore, the single microemulsion route follows the same principles explained above; after the incorporation of the second reactant, the process is controlled by one or more of the following mechanisms: reaction kinetics, particle aggregation, and intramicellar and/or intermicellar nucleation and growth. For instance, intramicellar routes will dominate when high reactant occupancy numbers are coupled with rigid surfactant layer, which is the desired condition to avoid particle aggregation. According to the literature [94, 99, 100], the use of surfactants with reactive counterions favors intermicellar nucleation and growth.

Similarly, there are several operation variables widely analyzed in the literature that can be controlled/modified to improve the reaction schemes of these approaches [94–98, 101–104], including dispersed phase/surfactant ratio, nature and concentration of surfactants, cosurfactants and reactive species, volume fraction and type of the dispersed and continuous phases, mixing, and temperature, among others.

1.3 Physical Preparation Techniques

Other preparation methods of nanoparticles are the top-down methods where nanoparticles are prepared directly from bulk materials via the generation of isolated atoms by using various distribution techniques that involve physical methods, such as milling or grinding, laser beam processing, repeated quenching, and photolithography [105]. Different nanoparticles preparation and characterization techniques and their effects on nanoparticles stability have been generously discussed by other researchers [106-119].

To name a few of these technologies, we can categorize these techniques as:

(i) Mechanical attrition, like attrition ball mill, planetary ball mill, vibrating ball mill, low energy tumbling mill, and high energy ball mill
(ii) Plasma
(iii) Microwave irradiation
(iv) Pulsed laser method
(v) Gamma radiation

A discussion on the first two techniques, as they are important ones, is addressed below.

1.3.1 Mechanical Attrition

Mechanical attrition, or "milling", is a process in which a device is used to apply energy to a coarse-grained structure, resulting in the reduction in particle size. Under certain conditions, mechanical attrition may result in nanoparticles which also exhibit nanostructural behavior due to the nanocrystallinity of the resulting material [120]. In the attrition process, the media is usually placed between two colliding balls, where the media is then subjected to an impact process reducing its size. During the process of attrition, the material, which usually contains large spaces compared to the particle size, undergoes three stages: The first stage is rearrangement of the particles, as particles slide past each one another with minimum fracture, followed by second stage of elastic and plastic deformation, and finally particle fracture.

There are several devices that can be used for mechanical alloying, which can be used for different applications (e.g., sample sizes, milled materials, etc.). These devices include the followings.

1.3.1.1 Shaker Mills

The sample is deposited in a vial that contains a grinding media, which are hard spheres. The shaking of the vial is accompanied by a lateral movement, both at several thousand times per minute. Due to the high speed of the hard spheres, the method is classified under the high-energy methods. These devices are usually used in laboratories, and for small amount of powder samples [120].

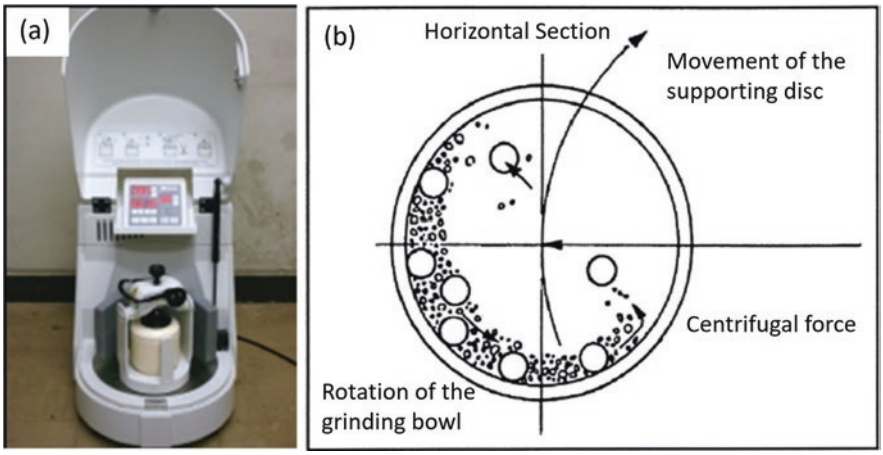

Fig. 1.11 (**a**) Planetary ball mill and (**b**) schematic showing motion of ball motion inside the grinding jar. (Adapted from [121] with permission)

1.3.1.2 Planetary Ball Mills

In this setup, shown schematically in Fig. 1.11, grinding jars or vials, which contain grinding hard spheres and the sample, are attached to a rotating disk (sun wheel). The vials rotate around their own axis and are subjected to the rotation of the sun wheel, which rotates in an opposite direction. This motion results in impact and friction forces on the hard spheres, causing a high degree of sample size reduction. These mills are also used in laboratories, but for larger sample sizes compared to shaker mills [121].

1.3.1.3 Attritor Mills

The mill consists of a drum filled with hard spheres, the powder sample, and an agitator. The milling is produced by the rotation of an agitator, which is a rotating vertical shaft with arm (impellers) attached at right angles. This rotation results in various impacts within the drum, including impacts among the hard spheres, the spheres, and the impellers and the walls, which finally lead to grinding the powder and reducing its size [120].

1.3.2 Plasma

One of the most common techniques for the preparation of supported metal/metal oxide nanoparticles as catalysts is wet process (including impregnation and precipitation), which is usually employed for economic and practical reasons. In contrast to these techniques, dry processes (including chemical/physical vapor deposition,

sputtering, and ion implantation) remain limited as catalytic nanoparticles preparation techniques. These methods specifically are applied in the emerging field of semiconductor technology. Although the science behind dry processes is important from a fundamental point of view, dry processes that enable the use of powdered catalyst nanomaterials for practical applications are not well-known.

Plasma has been used for catalyst nanomaterials preparation [122–125]. Various types of thermal and cold plasmas, including not limited to plasma jets, DC coronas, arcs, glow discharges, radio frequencies, and microwaves, have been employed for preparation of ultrafine particles including nanoparticles, supported catalysts, and/or catalyst surfaces modification. The potential advantages of using plasmas are (1) preparation of highly dispersed active species, (2) enhanced catalyst activation, selectivities, and lifetimes, (3) reduced energy requirements, and (4) shortened preparation times [124]. One of the promising techniques in this category can be named as pulsed cathodic arc plasma technique, which is a simple and innovative approach toward preparation of nanoparticles. This method enables the deposition of metal nanoparticles or nanofilms from bulk metals or other electronic conducting materials [126–142]. One of the most important applications of pulsed cathodic arc plasma technique is preparation of powdered-supported catalysts and photocatalysts. This method enables the one-step deposition of catalyst nanoparticles on various support powders, in contrary to the multistep preparation needed for conventional wet impregnation processes. A schematic and a photograph of the experimental setup for nanoparticle catalyst preparation using pulsed arc plasma deposition have been depicted in Fig. 1.12. This apparatus consists of arc discharge sources, a vacuum chamber with a turbomolecular pumping system, and a powder container with a rotating stirring mechanism. In the arc discharge source unit, an insulator tube, a columnar cathode, a trigger electrode, and a cylindrical anode are arranged coaxially. Cathode is a 10-mm-diameter and 17 -mm-long metal rod of the target material connected to a DC supply, while cylindrical anode is connected to the ground [143]. Trigger electrode in this case is connected to a pulsed power supply.

For the sake of charge and discharge, an electrolytic capacitor is connected between the cathode and the ground. An electronic breakdown between the trigger and cathode electrodes is caused by the application of a 3 kV pulse to the trigger electrode. This electronic breakdown ignites pulsed arc discharges with a period of 0.1 to 0.2 ms between the cathode and the anode.

Transmission electron microscopy (TEM) images and energy-dispersive X-ray spectroscopy (EDX) spectra of unsupported Pd–Fe nanoparticles prepared by (left) synchronous (syn) and (right) asynchronous (asyn) pulsing have been demonstrated in Fig. 1.13. As seen in this picture, each EDX spectrum was taken from a circular region containing one nanoparticle. In synchronous pulsing, the as-deposited single nanoparticles contained both Pd and Fe (Fe: 67 wt%, Pd: 33 wt%), whereas the single nanoparticles prepared via asynchronous pulsing contained only Fe (Fe: 100 wt%, Pd: 0 wt%) [143].

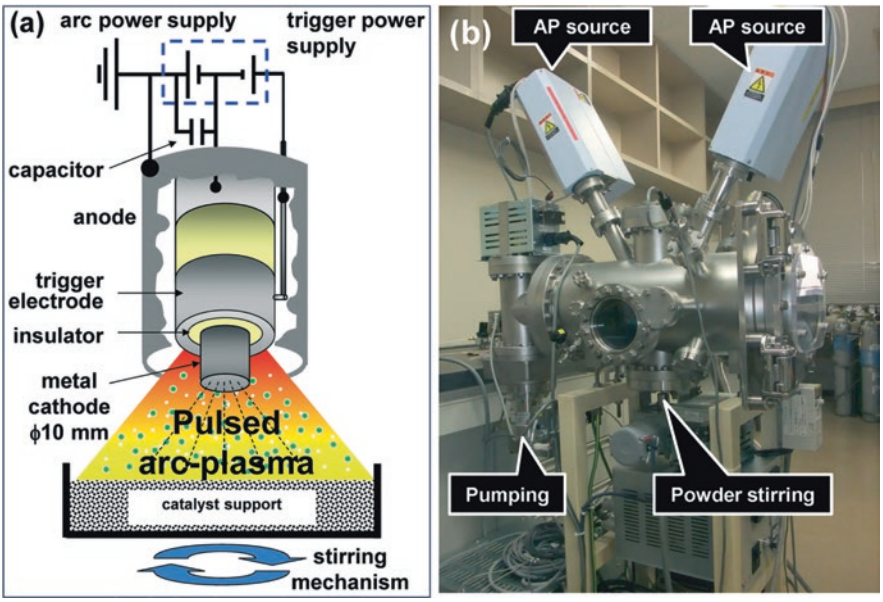

Fig. 1.12 (**a**) Schematic of the pulsed arc plasma process for the deposition of metal nanoparticles and (**b**) experimental setup with dual arc plasma sources. (Reproduced from [143] with permission from The Royal Society of Chemistry)

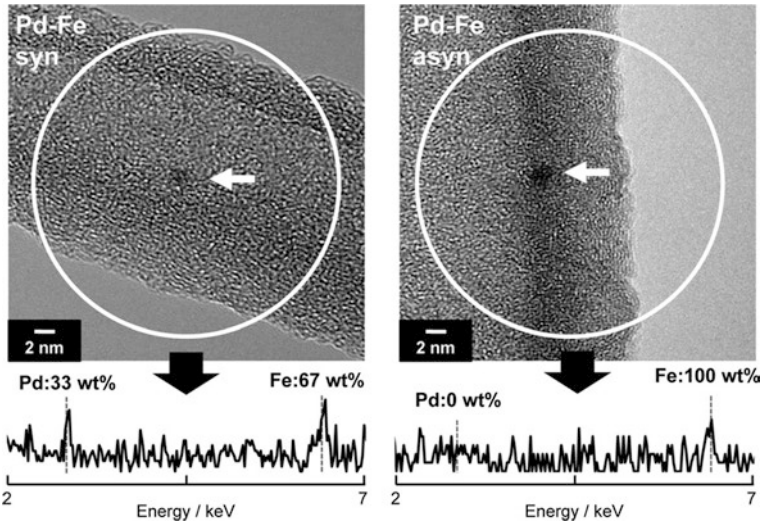

Fig. 1.13 TEM images and EDX spectra of unsupported Pd–Fe nanoparticles prepared by (left) synchronous (syn) and (right) asynchronous (asyn) pulsing. Each EDX spectrum was taken from a circular region containing one nanoparticle. (Reproduced from [143] with permission from The Royal Society of Chemistry)

1.4 Application: Importance of Controlling the Shape and Size of Nanoparticles

Nanotechnology is concerned with understanding the correlation between the chemical, optical, electrical, and magnetic properties of nanomaterials with respect to their size, shape, and surface chemistry [144]. The importance of the size is highlighted in the very definition of nanotechnology which, according to the National Nanotechnology Initiative (NNI), is the "*science, engineering, and technology conducted at the nanoscale, which is about 1 to 100 nm*" [145]. Once we are in the nanoparticle size range, the function of the nanoparticle size plays an equally important role as material properties (e.g., chemical and magnetic) become size-dependent and, therefore, a desired nanoparticle function is closely related to the nanoparticle size. To highlight the size and shape effects, we briefly go over a selected few field applications, but we emphasize that size and shape effects are present in all applications.

1.4.1 Metallurgy

Following observations regarding the effect of the size of small particle on melting temperature, Buffat and Borel [146] studied the melting temperature of gold particles of various sizes and found, using scanning electron-diffraction, that melting temperature increases with increasing particle size (see Fig. 1.14). Later, [147] highlighted what is known as *cluster size equations*, which included energetic, quantum, electronic, and electrodynamic size effects of the clusters.

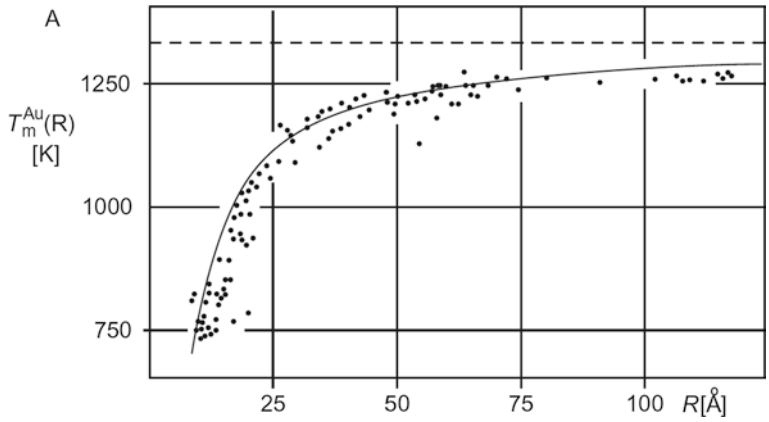

Fig. 1.14 Effect of gold nanoparticle size on the melting temperature. Adapted from [146, 147] with permission

1.4.2 Biological Systems

One way to explore the size and shape effects of nanoparticles is to look at these effects in naturally occurring biological nanostructures. Viruses, which are nanosized entities, exist in different shapes such as filamentous, isometric (or icosahedral), head and tail, and enveloped, and their ability to infect a certain cell type and their residence time in the infected cell are impacted by their shape [144]. The combined effect of shape and size can be noticed in the therapeutics used for degenerated (e.g., osteoarthritic) cartilage, where the molecule's size is the most important factor in the design of therapeutics, as the effective pore size in the matrix of the cartilage is very small (~6 nm). Surprisingly, certain molecules of larger hydrodynamic radius (e.g., 500 kDa dextran with ~16 nm) can penetrate and diffuse through cartilage. It is hypothesized that the linear shape of the dextran molecule enables it to penetrate and diffuse within pores of smaller size, while spherical molecules of similar hydrodynamic radius cannot penetrate cartilage [148]. Currently, therapies of degenerated cartilage are based on drugs of small hydrodynamic radius, which have limited long-term efficacy, and thus, the ability to inject cartilage with drugs of larger molecules that can penetrate the tissue could substantially improve the health of the degenerated tissue, but would also require knowing the size and shape, among other factors. Antigens and proteins are other examples of nanostructures whose functions are impacted by size and shape [144]. These examples of naturally occurring nanostructures demonstrate the importance of both size and shape, and that for designing synthetic nanoparticles for biological applications, e.g., detecting and repairing infected cells, tumor diagnosis, or drug delivery, physical properties play a detrimental role in the application, as they impact the interaction between nanoparticle and the cell surface (see Fig. 1.15). For instance, for tumor targeting nanoparticles, Perrault et al. [149] have shown that the permeation of the nanoparticles within a tumor, as well as their tumor accumulation capacity, is highly influenced by the nanoparticle's diameter, where smaller nanoparticles are able to diffuse throughout the tumor matrix.

1.4.3 Oil Well Construction

In oil well construction, cements experience volume shrinkage, which impacts the long-term stability of the wells and leads to gas leakage [150]. To reduce the effect of the shrinkage, certain additives, including nanoparticles, can be used. For instance, nanoscale magnesium oxide (MgO) is used as an additive in the cement slurry, expanding as it is converted to magnesium hydroxide once it is exposed to the water in the slurry and thus, reducing the shrinkage. The expansion properties are influenced by the surface area of the MgO particles, i.e., MgO particle size [151]. In the same topic, cements experience what is known as "waiting on cement" (WOC), which is the amount of time it takes the slurry to solidify. This waiting time

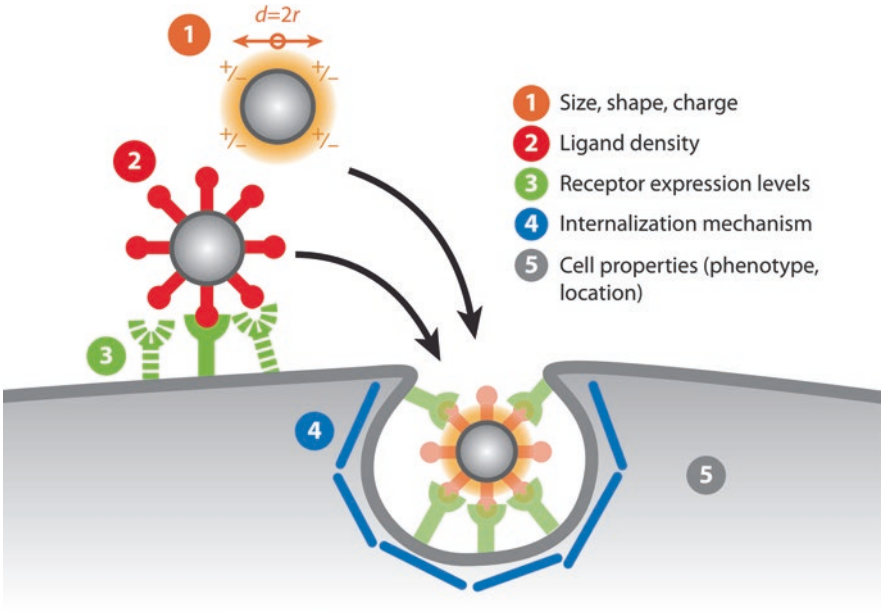

Fig. 1.15 Factors that impact nanoparticle and cell surface interaction. Adapted from reference [144] after permission

can be costly and is generally minimized by additives, or *cement accelerators*. Nanosilica has been shown to increase strength of the cement and decrease porosity, making it a favorable additive over other accelerators [152, 153]. Different sizes and shapes of nanosilica lead to different results [154]. For instance, the smallest nanosilica (5 nm in diameter), and the rod-shaped nanosilica exhibited the fastest rates of cement setting [151].

Tough well conditions and cement material issues can lead to debonding of the cement from the casing or the rock formation in the wellbore and the fracturing of the bulk cement, as has been proven with previous studies [151], as depicted in Figs. 1.16 and 1.17. Nanoparticles which have shown substantial promise in improving the properties of oil and gas well cement can be named as nanosilicas, calcium-silicate-hydrate (C-S-H) nanofoils, and nanomagnesia [151].

It should be noted that several other factors, besides size and shape, play significant roles on the function and kinetics of nanoparticles, such as magnetic field, mechanical properties, and pH effect, considering their applications.

1.4.4 Nanotechnology: Industrial Applications and Risk Factors

Over the past few decades, nanotechnology has infiltrated almost all research fields and introduced unconventional solutions to the current industrial problems. However, most of these solutions have not fully transitioned from the experimental

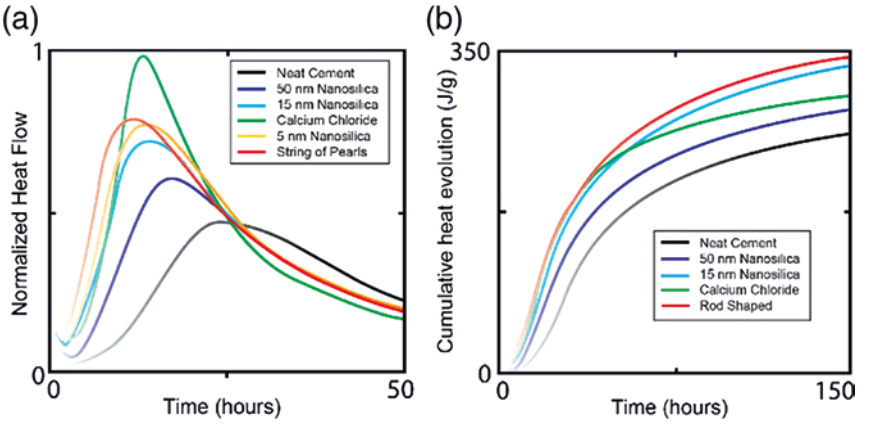

Fig. 1.16 Hydration kinetics of class H cement (**a**) heat flow and (**b**) cumulative heat, showing the effect of shape and size. (Adapted from [151] with permission)

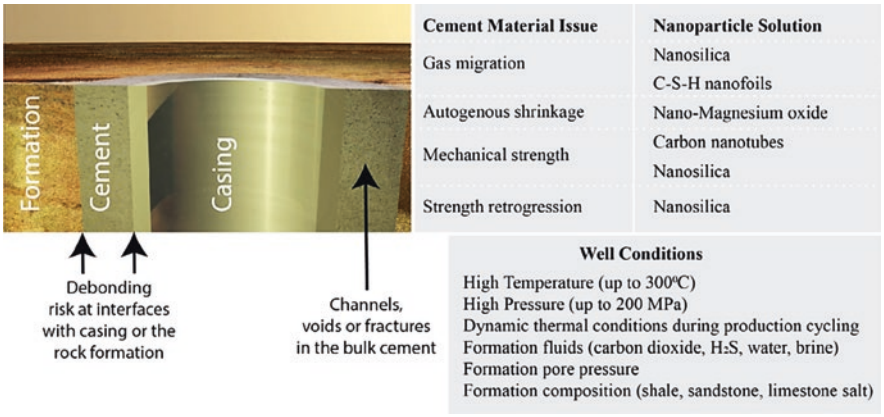

Fig. 1.17 Oil well construction materials and nanosolutions. (Adapted from [151] with permission)

laboratory stage to the industrial stage. With the rapid increase in the applications of nanotechnology in the industry, there are risks, concerns, and challenges attached to its use. In the following, we address some of the applications of nanotechnology along with potential risks. While we focus on two sectors, food industry and oil and gas, similar risks are also present in the other sectors.

1.4.4.1 Food Industry

Nanotechnology has recently attracted much attention in the food and beverage packaging industry, where there are several benefits of using engineered nanoparticles (ENP) in food-contact applications. However, such applications are also

accompanied by health concerns. While traditional packaging is mainly concerned with product preservation, nanotechnology is involved in *active* packaging, which extends the roles of packaging from the *inert* containment of the product to the *active* containment, which targets the improvement of nutrient and flavor delivery, and extends its shelf life [155]. According to the European regulation (EC) No 450/2009, active packaging technologies are designed to deliberately incorporate components that would release or absorb substances into or from the packaged food or the environment surrounding the food. Active packaging technologies include releasing systems (e.g., carbon dioxide) and absorbing systems such as oxygen scavengers, which can be used for products like cooked meat, or bakery products, and prevent them from discoloration and mold growth, as well as moisture scavengers, which extend shelf life by preserving moisture in products like fresh meat and certain fruits. For instance, Mu et al. [156] introduced an oxygen scavenging technology based on iron nanoparticles blended with active carbon, calcium chloride, and sodium chloride, which showed superior performance to its counterpart technology that utilizes microsized iron powder, in terms of both scavenging rate and capacity. Although there has been active packaging products (e.g., sachets and absorbent pads), the primary challenge in the commercialization of these technologies is the health risk they pose as the active additives, e.g., nanoparticles, could migrate from the packaging into the product by means of diffusion from higher concentration (package) into lower concentration (food) [157]. A schematic of absorbent pad architecture has been depicted in Fig. 1.18 [159].

Moreover, due to their size, nanoparticles can navigate the body (cells, tissues, and organs) much more easily compared to microsized particles. As a result, there

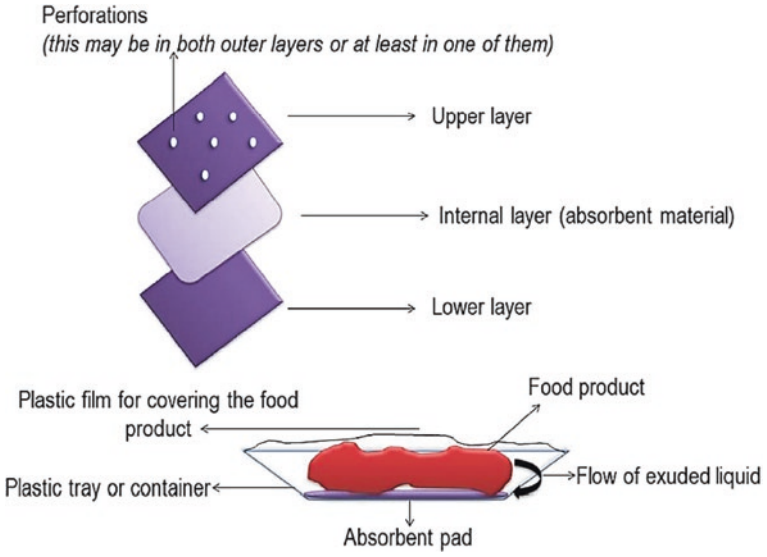

Fig. 1.18 Architecture of absorbent pad. (Adapted from [159] with permission)

has been a tendency for studying the interaction between the food matrix and the engineered nanoparticles. To address this issue, the conditions under which nanoparticles migrate need to be studied. Zhang et al. [158] introduced a standardized food model for the evaluation of the effect of food matrix on the toxicity and fate of ingested nanoparticles, and the study looked into titanium dioxide nanoparticles, a common food additive.

1.4.4.2 Oil and Gas

Recently, there has been extensive research on using nanotechnology in different aspects of the oilfield industry, including drilling, reservoir completion, enhanced oil upgrading and recovery, and produced water treatment, to name a few. The need for new technologies is fueled by the fact that the current resources are diminishing quickly, and therefore, such resources need to be well utilized. However, many of the proposed technologies, which are in their experimental stage, face many challenges, which hinder their applicability to the industry. Two of the main challenges are listed below.

1.4.5 Upscaling from Laboratory to Industry

When scaling up to meet the industrial demand, the level of control over the nanoparticle size, which would be feasible at the nanoscale, becomes more difficult to achieve, which is reflected on the properties of the synthesized matter [160]. This also is accompanied by the high cost and time that come with using nanoparticles at the industrial level, in addition to the inconsistent performance which may result from using several batches. As a result, processes for synthesizing nanoparticles at an industrial scale need to be developed, which is another challenge as this would require having the industry invest in developing such processes. In oil and gas industry, different additional challenges depend on the application. A summary of some of the key challenges is provided in Table 1.1 [160].

1.4.6 Health and Safety Risks

The nature of the nanostructure plays an important role in risk assessment. Nanoparticles that are incorporated into a substance (e.g., nanocomposite and nanocomponents) are referred to as *fixed* nanoparticles and pose lower risk than *free* nanoparticles, which are individual nanoparticles. For instance, in oil and gas applications, free nanoparticles could be injected into the wellbore with the enhanced-oil-recovery fluids. Although the effect of nanoparticles on the body is still to be studied, if they enter the body, e.g., by inhaling, absorption, or skin contact, they

Table 1.1 Nanotechnology applications in oilfield and attached challenges adopted with permission from [160]

Nanotechnology	Nano tool	Oilfield application	Key challenges
Nano electronics	Nano sensors	Reservoir and flood front imaging	Long battery life under reservoir conditions
Nano optics	Quantum dots	Logging	Transport through reservoir
Nano magnetism	Ferrofluids	Reservoir/ fracture imaging	Development of MNP, EM sources and receivers, data acquisition and signal processing software
	Magnetic nanoparticles	Produced water (PW) treatment	Scale up from lab to field
Nano composites and fibers	Single wall carbon tube, fullerenes, multiwall carbon tube	New casing and tubing materials, drill bits, proppants	Constructing and testing prototype
Surface active nanoparticles	Functionalized nanoparticles	EOR	Transport through reservoir
Nanoencapsulation	Chemical-laden nanoparticles, Biodegradable polymeric nanoparticles, phase inversion nanoencapsulation	Acid stimulation, profile control, gas mobility control	Scale up from lab to field
Nano thin film	Nanocomposite coatings	Drill bits, drilling fluids, completion fluids, shale inhibition	Construction and testing prototype
Nanocatalyst	Nickel nanoparticles	Catalyst for *in situ* thermal upgrading of heavy oil	Transport through reservoir, scale up

trigger an immune response and cause an overload of phagocytes (cells that destroy and devour pathogens). Moreover, they may interfere with the biological processes, which is made worse due to their large surface-area-to-volume ratio posing higher risk than their counterpart microsized particles [161]. In addition to the safety risks, there are several environmental risks of using nanoparticles at an industrial scale. A thorough review of challenges and uncertainties of using nanoparticles in oil and gas applications and associated risk factors will be addressed in detail in Chap. 15 of this book.

1.5 Conclusion

Nanoparticles, being a byproduct of industrial revolution, have great potential in changing the way humans connect to the world in the modern era. Nanoparticles have special physical properties distinct from both molecular and solid-state matter due to their significant fraction of surface atoms. Study of these physical properties provides us a unique way to learn how nanoparticles can be prepared and characterized. Knowledge of the application of nanoparticles in different industrial settings dictates nanoparticle preparation techniques and characterization. Knowledge of diverse application of these nanomaterials in the oil and gas industry from exploration and production to refinery, dictates urgent need for advanced preparation techniques and characterization.

Nanoparticle preparation techniques can be categorized into two main categories of chemical and physical techniques. Chemical pathway, also known as bottom-up technique, involves molecular components as starting materials linked with chemical reactions, nucleation, and growth processes to promote the formation of nanoparticles. Chemical coprecipitation, electrochemical, sonochemical, sol-gel processing, chemical vapor deposition, chemical vapor condensation, and (w/o) microemulsions are only a few of these methods. On the other hand, physical preparation methods, known as top-down methods, imply the preparation of nanoparticles via generation of isolated atoms by using various distribution techniques that involve physical methods, such as milling or grinding, laser beam processing, repeated quenching, photolithography, pulsed laser techniques, and plasma techniques, whose recent advances have been reviewed briefly in this chapter. Later, importance of controlling the shape and size of nanoparticles considering their application has been generally reviewed. In the last part of this chapter, industrial applications and risks/challenges associated with the advancements of nanotechnology have been briefly discussed.

Over the past few decades, nanotechnology has found its way in almost all research fields, and introduced unconventional solutions to the current industrial problems; however, most of these solutions have not fully transitioned from the experimental laboratory stage to the industrial stage. With the rapid enhanced applications of nanotechnology in the industry, there are risks, concerns, and challenges attached to its use, which are still somehow not known or under investigation. In the last section, we addressed some of the applications of nanotechnology along with its potential risks/challenges. While we focus on two sectors, food industry and oil and gas, similar risks are also present in the other sectors. Facing the fast-paced advancement of nanotechnology in almost every industry, we need to be aware and adopt ourselves in unconventional and out of the box thinking methods toward novel solutions, as modern problems solutions dictate a novel way of thinking.

References

1. National Nanotechnology Initiative (NNI). National Science and Technology Council. Committee on Technology, Subcommittee on Nanoscale Science, National Technology Initiative Strategic Plan, www.nano.gov (2011, Accessed 25 Aug 2015)
2. S. Iijima, Helical microtubules of graphitic carbon. Nature **354**, 56–58 (1991)
3. M. Boutonnet, J. Kizling, P. Stenius, Colloids Surf. **5**, 209 (1982)
4. A. Nasir, A. Kausar, A. Younus, A review on preparation, properties and applications of polymeric nanoparticle-based materials. Polym. Plastics Technol. Eng. **54**(4), 325–341 (2015). https://doi.org/10.1080/03602559.2014.958780
5. R. Francis, N. Joy, E.P. Aparna, R. Vijayan, Polymer grafted inorganic nanoparticles, preparation, properties, and applications: A review. Polym. Rev. **54**, 268–347 (2014)
6. Y. Zhang, Z. Chen, Z. Dong, M. Zhao, S. Ning, P. He, Preparation of raspberry-like adsorbed silica nanoparticles via miniemulsion polymeri- zation using a glycerol-functionalized silica sol. Int. J. Polym. Mater. Polym. Biomater. **62**, 397–401 (2013)
7. J.P. Rao, K.E. Geckeler, Polymer nanoparticles: Preparation techniques and size-control parameters. Prog. Polym. Sci. **36**, 887–913 (2011)
8. X. Wang, J.E. Hall, S. Warren, J. Krom, J.M. Magistrelli, M. Rackaitis, G.G.A. Bohm, Synthesis, characterization, and application of novel polymeric nanoparticles. Macromolecules **40**, 499–508 (2007)
9. N.N. Nassar, Iron oxide nanoadsorbents for removal of various pollutants from wastewater: An overview. Appl. Adsorb. Water Pollut. Control, 81–118 (2012)
10. M. Globe, *Preparation and Characterization of Monodisperse Magnetite sols in W/O Microemulsion*. (1983)
11. C. Bock, C. Paquet, M. Couillard, G.A. Botton, B.R. MacDougall, Size-selected synthesis of PtRu nano-catalysts: Reaction and size control mechanism. J. Am. Chem. Soc. **126**(25), 8028–8037 (2004)
12. X. Pang, L. Zhao, W. Han, X. Xin, Z. Lin, A general and robust strategy for the synthesis of nearly monodisperse colloidal nanocrystals. Nat. Nanotechnol. **8**(6), 426–431 (2013)
13. M.M. Husein, N.N. Nassar, Nanoparticle preparation using the single microemulsions scheme. Curr. Nanosci. **4**(4), 370–380 (2008)
14. F. Sagala, *Naturally Derived Silicate-Based Nanoparticles for Enhanced Oil Recovery in Sandstone Reservoirs*. (2020)
15. L.C. Varanda, C.G.S.D. Souza, C.J. Perecin, D.A.D. Moraes, D.F.D. Queiróz, H.R. Neves, et al., Chapter 3 - Inorganic and organic–inorganic composite nanoparticles with potential biomedical applications: synthesis challenges for enhanced performance, in *Materials for Biomedical Engineering*, ed. by V. Grumezescu, A. M. Grumezescu, (Elsevier, 2019), pp. 47–99
16. M.O. Besenhard, A.P. LaGrow, A. Hodzic, M. Kriechbaum, L. Panariello, G. Bais, et al., Co-precipitation synthesis of stable iron oxide nanoparticles with NaOH: New insights and continuous production via flow chemistry. Chem. Eng. J. **399**, 125740 (2020)
17. J.W. Mullin, 8 - Industrial techniques and equipment, in *Crystallization*, ed. by J. W. Mullin, 4th edn., (Butterworth-Heinemann, Oxford, 2001), pp. 315–402
18. M. Lok, Coprecipitation, in *Synthesis of Solid Catalysts*, (Wiley, 2009), pp. 135–151
19. B.L. Cushing, V.L. Kolesnichenko, C.J. O'Connor, Recent advances in the liquid-phase syntheses of inorganic nanoparticles. Chem. Rev. **104**(9), 3893–3946 (2004)
20. Z. Wu, S. Yang, W. Wu, Shape control of inorganic nanoparticles from solution. Nanoscale **8**(3), 1237–1259 (2016)
21. A.E. Nielsen, Precipitation. Croat. Chem. Acta **42**(2), 319–333 (1970)
22. J.-P. Jolivet, M. Henry, J. Livage, *Metal Oxide Chemistry and Synthesis: From Solution to Solid State* (Wiley-Blackwell, 2000)
23. D.R. Lide, *CRC Handbook of Chemistry and Physics*, 87th edn. (Taylor & Francis, 2006)

24. C. Jia, Y. Cheng, F. Bao, D. Chen, Y. Wang, pH value-dependant growth of α-Fe2O3 hierarchical nanostructures. J. Cryst. Growth **294**(2), 353–357 (2006)
25. G. Pandey, S. Singh, G. Hitkari, Synthesis and characterization of polyvinyl pyrrolidone (PVP)-coated Fe3O4 nanoparticles by chemical co-precipitation method and removal of Congo red dye by adsorption process. Int. Nano Lett. **8**(2), 111–121 (2018)
26. A. Chitsaz, M. Jalilpour, M. Fathalilou, Effects of PVP and CTAB surfactants on the morphology of cerium oxide nanoparticles synthesized via co-precipitation method. Int. J. Mater. Res. **104**(5), 511–514 (2013)
27. A. Radoń, A. Drygała, Ł. Hawełek, D. Łukowiec, Structure and optical properties of Fe3O4 nanoparticles synthesized by co-precipitation method with different organic modifiers. Mater. Charact. **131**, 148–156 (2017)
28. D.-H. Chen, Y.-Y. Chen, Synthesis of strontium ferrite nanoparticles by coprecipitation in the presence of polyacrylic acid. Mater. Res. Bull. **37**(4), 801–810 (2002)
29. J. Peng, F. Zou, L. Liu, L. Tang, L. Yu, W. Chen, et al., Preparation and characterization of PEG-PEI/Fe3O4 nano-magnetic fluid by co-precipitation method. Trans. Nonferrous Metals Soc. China **18**(2), 393–398 (2008)
30. I. Riva'i, I.O. Wulandari, H. Sulistyarti, A. Sabarudin, Ex-situ synthesis of polyvinyl alcohol(PVA)-coated Fe3O4 nanoparticles by coprecipitation-ultrasonication method. IOP Conf. Ser. Mater. Sci. Eng. **299**, 012065 (2018)
31. S. Akbari, S.M. Masoudpanah, S.M. Mirkazemi, N. Aliyan, PVA assisted coprecipitation synthesis and characterization of MgFe2O4 nanoparticles. Ceram. Int. **43**(8), 6263–6267 (2017)
32. M. Anbarasu, M. Anandan, E. Chinnasamy, V. Gopinath, K. Balamurugan, Synthesis and characterization of polyethylene glycol (PEG) coated Fe3O4 nanoparticles by chemical co-precipitation method for biomedical applications. Spectrochim. Acta A Mol. Biomol. Spectrosc. **135**, 536–539 (2015)
33. Y. Zhang, Z. Nan, Modified magnetic properties of MnFe2O4 by CTAB with coprecipitation method. Mater. Lett. **149**, 22–24 (2015)
34. D. Varghese, C. Tom, C.N. Krishna, Effect of CTAB on structural and optical properties of CuO nanoparticles prepared by coprecipitation route. IOP Conf. Ser. Mater. Sci. Eng. **263**, 022002 (2017)
35. L. Shen, Y. Qiao, Y. Guo, S. Meng, G. Yang, M. Wu, et al., Facile co-precipitation synthesis of shape-controlled magnetite nanoparticles. Ceram. Int. **40**(1, Part B), 1519–1524 (2014)
36. T. Fuchigami, S. Inagi, M. Atobe, *Organic Electrode Reactions. Fundamentals and Applications of Organic Electrochemistry*. (2014), pp. 1–10 and 45–82
37. A. Serrà, E. Vallés, Advanced electrochemical synthesis of multicomponent metallic nanorods and nanowires: Fundamentals and applications. Appl. Mater. Today **12**, 207–234 (2018)
38. F. Nasirpouri, Fundamentals and principles of electrode-position, in *Electrodeposition of Nanostructured Materials*, ed. by F. Nasirpouri, (Springer International Publishing, Cham, 2017), pp. 75–121
39. U.S. Mohanty, Electrodeposition: A versatile and inexpensive tool for the synthesis of nanoparticles, nanorods, nanowires, and nanoclusters of metals. J. Appl. Electrochem. **41**(3), 257–270 (2011)
40. D. Bera, S.C. Kuiry, S. Seal, Synthesis of nanostructured materials using template-assisted electrodeposition. JOM **56**(1), 49–53 (2004)
41. M.T. Reetz, W. Helbig, Size-selective synthesis of nanostructured transition metal clusters. J. Am. Chem. Soc. **116**(16), 7401–7402 (1994)
42. N. Sato, Chapter 7 - electrode reactions, in *Electrochemistry at Metal and Semiconductor Electrodes*, ed. by N. Sato, (Elsevier Science, Amsterdam, 1998), pp. 213–233
43. F. Nasirpouri, An overview to electrochemistry, in *Electrodeposition of Nanostructured Materials*, ed. by F. Nasirpouri, (Springer International Publishing, Cham, 2017), pp. 43–73
44. A. Takai, Y. Yamauchi, K. Kuroda, Facile formation of single crystalline Pt nanowires on a substrate utilising lyotropic liquid crystals consisting of cationic surfactants. J. Mater. Chem. **19**(24), 4205–4210 (2009)

45. Y. Song, R.M. Garcia, R.M. Dorin, H. Wang, Y. Qiu, E.N. Coker, et al., Synthesis of platinum nanowire networks using a soft template. Nano Lett. **7**(12), 3650–3655 (2007)
46. Y. Imura, H. Tanuma, H. Sugimoto, R. Ito, S. Hojo, H. Endo, et al., Water-dispersible ultrathin au nanowires prepared using a lamellar template of a long-chain amidoamine derivative. Chem. Commun. **47**(22), 6380–6382 (2011)
47. X. Gao, F. Lu, B. Dong, Y. Liu, Y. Gao, L. Zheng, Facile synthesis of gold and gold-based alloy nanowire networks using wormlike micelles as soft templates. Chem. Commun. **51**(5), 843–846 (2015)
48. Q. Zhou, X. Liu, Y. Zhao, N. Jia, L. Liu, M. Yan, et al., Single crystal tin nano-rod arrays electrodeposited by a soft template. Chem. Commun. **39**, 4941–4942 (2005)
49. A. Serrà, E. Gómez, J.F. López-Barbera, J. Nogués, E. Vallés, Green electrochemical template synthesis of CoPt nanoparticles with Tunable size, composition, and magnetism from microemulsions using an ionic liquid (bmimPF6). ACS Nano **8**(5), 4630–4639 (2014)
50. I. Kaminska, M. Jonsson-Niedziolka, A. Kaminska, M. Pisarek, R. Hołyst, M. Opallo, et al., Electrodeposition of well-adhered multifarious au particles at a solid|toluene|aqueous electrolyte three-phase junction. J. Phys. Chem. C **116**(42), 22476–22485 (2012)
51. M. Pérez-Page, E. Yu, J. Li, M. Rahman, D.M. Dryden, R. Vidu, et al., Template-based syntheses for shape controlled nanostructures. Adv. Colloid Interf. Sci. **234**, 51–79 (2016)
52. D. Bera, S.C. Kuiry, S. Patil, S. Seal, Palladium nanoparticle arrays using template-assisted electrodeposition. Appl. Phys. Lett. **82**(18), 3089–3091 (2003)
53. A.J. Fragoso-Medina, F. López-Saucedo, G.G. Flores-Rojas, E. Bucio, Chapter 11 - Sonochemical synthesis of inorganic nanomaterials, in *Green Sustainable Process for Chemical and Environmental Engineering and Science*, ed. by B. R. Inamuddin, M. I. Ahamed, A. M. Asiri, (Elsevier, 2021), pp. 263–279
54. A. Gedanken, Using sonochemistry for the fabrication of nanomaterials. Ultrason. Sonochem. **11**(2), 47–55 (2004)
55. M. Kamali, R. Dewil, L. Appels, T.M. Aminabhavi, Nanostructured materials via green sonochemical routes – Sustainability aspects. Chemosphere **276**, 130146 (2021)
56. B.M. Teo, *Ultrasonic Synthesis of Polymer Nanoparticles. Handbook of Ultrasonics and Sonochemistry* (Springer, Singapore, 2016), pp. 365–393
57. H. Xu, B.W. Zeiger, K.S. Suslick, Sonochemical synthesis of nanomaterials. Chem. Soc. Rev. **42**(7), 2555–2567 (2013)
58. A. Gedanken, Ultrasonic Processing to Produce Nanoparticles, in *Encyclopedia of Materials: Science and Technology*, ed. by B. KHJ, R. W. Cahn, M. C. Flemings, B. Ilschner, E. J. Kramer, S. Mahajan, et al., (Elsevier, Oxford, 2001), pp. 9450–9456
59. A. Gedanken, I. Perelshtein, 18 - Power ultrasound for the production of nanomaterials, in *Power Ultrasonics*, ed. by J. A. Gallego-Juárez, K. F. Graff, (Woodhead Publishing, Oxford, 2015), pp. 543–576
60. J.H. Bang, K.S. Suslick, Applications of ultrasound to the synthesis of nanostructured materials. Adv. Mater. **22**(10), 1039–1059 (2010)
61. J. Lee, *Importance of Sonication and Solution Conditions on the Acoustic Cavitation Activity. Handbook of Ultrasonics and Sonochemistry* (Springer, Singapore, 2016), pp. 137–175
62. F. Mohandes, M. Salavati-Niasari, Sonochemical synthesis of silver vanadium oxide micro/nanorods: Solvent and surfactant effects. Ultrason. Sonochem. **20**(1), 354–365 (2013)
63. C.U. Okoli, K.A. Kuttiyiel, J. Cole, J. McCutchen, H. Tawfik, R.R. Adzic, et al., Solvent effect in sonochemical synthesis of metal-alloy nanoparticles for use as electrocatalysts. Ultrason. Sonochem. **41**, 427–434 (2018)
64. M. D'Arienzo, R. Scotti, B. Di Credico, M. Redaelli, Chapter 13 - Synthesis and characterization of morphology-controlled TiO2 nanocrystals: Opportunities and challenges for their application in photocatalytic materials, in *Studies in Surface Science and Catalysis*, ed. by P. Fornasiero, M. Cargnello, (Elsevier, 2017), pp. 477–540
65. R.C. Mehrotra, Synthesis and reactions of metal alkoxides. J. Non-Cryst. Solids **100**(1), 1–15 (1988)

66. T. Athar, Chapter 17 - Smart precursors for smart nanoparticles, in *Emerging Nanotechnologies for Manufacturing*, ed. by W. Ahmed, M. J. Jackson, 2nd edn., (William Andrew Publishing, Boston, 2015), pp. 444–538
67. M. Parashar, V.K. Shukla, R. Singh, Metal oxides nanoparticles via sol–gel method: A review on synthesis, characterization and applications. J. Mater. Sci. Mater. Electron. **31**(5), 3729–3749 (2020)
68. L.L. Hench, J.K. West, The sol-gel process. Chem. Rev. **90**(1), 33–72 (1990)
69. U. Schubert, *Chemistry and Fundamentals of the Sol–Gel Process. The Sol-Gel Handbook*. (2015), pp. 1–28
70. M. Henry, J.P. Jolivet, J. Livage, Aqueous chemistry of metal cations: Hydrolysis, condensation and complexation, in *Chemistry, Spectroscopy and Applications of Sol-Gel Glasses*, ed. by R. Reisfeld, C. K. Jjørgensen, (Springer, Berlin/Heidelberg, 1992), pp. 153–206
71. *Hydrolysis of Metal Alkoxides and Synthesis of Simple Oxides by The Sol-Gel Method. The Chemistry of Metal Alkoxides*, (Springer, Boston, 2002), pp. 107–25
72. D.M. Smith, R. Deshpande, B.C. Jeffrey, Preparation of low-density aerogels at ambient pressure. MRS Proc. **271**, 567 (1992)
73. S.S. Ray, R. Gusain, N. Kumar, Chapter four - Adsorption in the context of water purification, in *Carbon Nanomaterial-Based Adsorbents for Water Purification*, ed. by S. S. Ray, R. Gusain, N. Kumar, (Elsevier, 2020), pp. 67–100
74. V. Purcar, V. Rădiţoiu, A. Dumitru, C.-A. Nicolae, A.N. Frone, M. Anastasescu, et al., Antireflective coating based on TiO2 nanoparticles modified with coupling agents via acid-catalyzed sol-gel method. Appl. Surf. Sci. **487**, 819–824 (2019)
75. S. Cai, Y. Zhang, H. Zhang, H. Yan, H. Lv, B. Jiang, Sol–gel preparation of hydrophobic silica antireflective coatings with low refractive index by base/acid two-step catalysis. ACS Appl. Mater. Interfaces **6**(14), 11470–11475 (2014)
76. S.V. Lazareva, N.V. Shikina, L.E. Tatarova, Z.R. Ismagilov, Synthesis of high-purity silica nanoparticles by sol-gel method. Eurasian Chem. Technol. J. **19**(4), 295–302 (2017)
77. S.A. Ibrahim, S. Sreekantan, Effect of pH on TiO2 nanoparticles via sol-gel method. Adv. Mater. Res. **173**, 184–189 (2011)
78. S. Hosseini Largani, P.M. Akbarzadeh, The effect of concentration ratio and type of functional group on synthesis of CNT–ZnO hybrid nanomaterial by an in situ sol–gel process. Int. Nano Lett. **7**(1), 25–33 (2017)
79. M.S. Tokumoto, S.H. Pulcinelli, C.V. Santilli, V. Briois, Catalysis and temperature dependence on the formation of ZnO nanoparticles and of zinc acetate derivatives prepared by the sol−gel route. J. Phys. Chem. B **107**(2), 568–574 (2003)
80. K.L. Choy, Chapter 12 - Vapor processing of nanostructured materials, in *Handbook of Nanostructured Materials and Nanotechnology*, ed. by H. S. Nalwa, (Academic Press, Burlington, 2000), pp. 533–577
81. L. Sun, G. Yuan, L. Gao, J. Yang, M. Chhowalla, M.H. Gharahcheshmeh, et al., Chemical vapour deposition. Nat. Rev. Methods Primers **1**(1), 5 (2021)
82. Chapter 1 Overview of Chemical Vapour Deposition, in *Chemical Vapour Deposition: Precursors, Processes and Applications. The Royal Society of Chemistry*, ed. by A. C. Jones, M. L. Hitchman, (2009), pp. 1–36
83. W. Chang, G. Skandan, S.C. Danforth, B.H. Kear, H. Hahn, Chemical vapor processing and applications for nanostructured ceramic powders and whiskers. Nanostruct. Mater. **4**(5), 507–520 (1994)
84. A. Tavakoli, M. Sohrabi, A. Kargari, A review of methods for synthesis of nanostructured metals with emphasis on iron compounds. Chem. Pap. **61**(3), 151–170 (2007)
85. Y.M. Manawi, S.A. Ihsanullah, T. Al-Ansari, M.A. Atieh, A review of carbon nanomaterials' synthesis via the Chemical Vapor Deposition (CVD) method. Materials **11**(5) (2018)
86. H. Lee, M.Y. Song, J. Jurng, Y.-K. Park, The synthesis and coating process of TiO2 nanoparticles using CVD process. Powder Technol. **214**(1), 64–68 (2011)

87. M. Kumar, Y. Ando, Chemical vapor deposition of carbon nanotubes: A review on growth mechanism and mass production. J. Nanosci. Nanotechnol. **10**(6), 3739–3758 (2010)
88. M. Meyyappan, A review of plasma enhanced chemical vapour deposition of carbon nanotubes. J. Phys. D. Appl. Phys. **42**(21), 213001 (2009)
89. J. Ramanujam, A. Verma, Photovoltaic properties of a-Si:H films grown by plasma enhanced chemical vapor deposition: A review. Mater. Express **2**(3), 177–196 (2012)
90. L. Martinu, O. Zabeida, J.E. Klemberg-Sapieha, Chapter 9 - Plasma-enhanced chemical vapor deposition of functional coatings, in *Handbook of Deposition Technologies for Films and Coatings*, ed. by P. M. Martin, 3rd edn., (William Andrew Publishing, Boston, 2010), pp. 392–465
91. C.A. Dorval Dion, J.R. Tavares, Photo-initiated chemical vapor deposition as a scalable particle functionalization technology (a practical review). Powder Technol. **239**, 484–491 (2013)
92. Y. van de Burgt, Laser-assisted growth of carbon nanotubes—A review. J. Laser Appl. **26**(3), 032001 (2014)
93. A.P. Caricato, A. Luches, Applications of the matrix-assisted pulsed laser evaporation method for the deposition of organic, biological and nanoparticle thin films: A review. Appl. Phys. A **105**(3), 565–582 (2011)
94. M.M. Husein, N.N. Nassar, Nanoparticle preparation using the single microemulsions scheme. Curr. Nanosci. **4**(4), 370–380 (2008)
95. A.K. Ganguli, A. Ganguly, S. Vaidya, Microemulsion-based synthesis of nanocrystalline materials. Chem. Soc. Rev. **39**(2), 474–485 (2010)
96. S. Wolf, C. Feldmann, Microemulsions: Options to expand the synthesis of inorganic nanoparticles. Angew. Chem. Int. Ed. **55**(51), 15728–15752 (2016)
97. M. Sanchez-Dominguez, K. Pemartin, M. Boutonnet, Preparation of inorganic nanoparticles in oil-in-water microemulsions: A soft and versatile approach. Curr. Opin. Colloid Interface Sci. **17**(5), 297–305 (2012)
98. J.-P. Ge, W. Chen, L.-P. Liu, Y.-D. Li, Formation of disperse nanoparticles at the oil/water interface in normal microemulsions. Chem. Eur. J. **12**(25), 6552–6558 (2006)
99. M. Husein, E. Rodil, J.H. Vera, Formation of silver bromide precipitate of nanoparticles in a single microemulsion utilizing the surfactant counterion. J. Colloid Interface Sci. **273**(2), 426–434 (2004)
100. M.M. Husein, E. Rodil, J.H. Vera, Preparation of AgBr nanoparticles in microemulsions via reaction of AgNO3 with CTAB counterion. J. Nanopart. Res. **9**(5), 787–796 (2007)
101. J. Eastoe, M.J. Hollamby, L. Hudson, Recent advances in nanoparticle synthesis with reversed micelles. Adv. Colloid Interface Sci. **128–130**, 5–15 (2006)
102. M.A. Malik, M.Y. Wani, M.A. Hashim, Microemulsion method: A novel route to synthesize organic and inorganic nanomaterials: 1st Nano Update. Arab. J. Chem. **5**(4), 397–417 (2012)
103. J.N. Solanki, Z.V.P. Murthy, Controlled size silver nanoparticles synthesis with water-in-oil microemulsion method: A topical review. Ind. Eng. Chem. Res. **50**(22), 12311–12323 (2011)
104. M.A. López-Quintela, J. Rivas, M.C. Blanco, C. Tojo, Synthesis of nanoparticles in microemulsions, in *Nanoscale Materials*, ed. by L. M. Liz-Marzán, P. V. Kamat, (Springer, Boston, 2003), pp. 135–155
105. C.M. Niemeyer, Nanoparticles, proteins, and nucleic acids: Biotechnology meets materials science. Angew. Chem. Int. Ed. **40**(22), 4128–4158 (2001)
106. J. Jiang, G. Oberdörster, P. Biswas, Characterization of size, surface charge, and agglomeration state of nanoparticle dispersions for toxicological studies. J. Nanopart. Res. **11**(1), 77–89 (2009)
107. A. Ghadimi, R. Saidur, H. Metselaar, A review of nanofluid stability properties and characterization in stationary conditions. Int. J. Heat Mass Transf. **54**(17–18), 4051–4068 (2011)
108. L. Wu, J. Zhang, W. Watanabe, Physical and chemical stability of drug nanoparticles. Adv. Drug Deliv. Rev. **63**(6), 456–469 (2011)
109. C. Lourenco, M. Teixeira, S. Simões, R. Gaspar, Steric stabilization of nanoparticles: Size and surface properties. Int. J. Pharm. **138**(1), 1–12 (1996)

110. M. Iijima, H. Kamiya, Surface modification for improving the stability of nanoparticles in liquid media. KONA Powder Particle J. **27**, 119–129 (2009)
111. H. ShamsiJazeyi, C.A. Miller, M.S. Wong, J.M. Tour, R. Verduzco, Polymer-coated nanoparticles for enhanced oil recovery. J. Appl. Polym. Sci. **131**(15) (2014)
112. M. Ranka, P. Brown, T.A. Hatton, Responsive stabilization of nanoparticles for extreme salinity and high-temperature reservoir applications. ACS Appl. Mater. Interfaces **7**(35), 19651–19658 (2015)
113. D.A. Ersenkal, A. Ziylan, N.H. Ince, H.Y. Acar, M. Demirer, N.K. Copty, Impact of dilution on the transport of poly (acrylic acid) supported magnetite nanoparticles in porous media. J. Contam. Hydrol. **126**(3), 248–257 (2011)
114. C. Barrera, A.P. Herrera, N. Bezares, E. Fachini, R. Olayo-Valles, J.P. Hinestroza, C. Rinaldi, Effect of poly (ethylene oxide)-silane graft molecular weight on the colloidal properties of iron oxide nanoparticles for biomedical applications. J. Colloid Interface Sci. **377**(1), 40–50 (2012)
115. N. Jain, Y. Wang, S.K. Jones, B.S. Hawkett, G.G. Warr, Optimized steric stabilization of aqueous ferrofluids and magnetic nanoparticles. Langmuir **26**(6), 4465–4472 (2009)
116. P.L. Golas, S. Louie, G.V. Lowry, K. Matyjaszewski, R.D. Tilton, Comparative study of polymeric stabilizers for magnetite nanoparticles using ATRP. Langmuir **26**(22), 16890–16900 (2010)
117. A. Tiraferri, K.L. Chen, R. Sethi, M. Elimelech, Reduced aggregation, and sedimentation of zero-valent iron nanoparticles in the presence of guar gum. J. Colloid Interface Sci. **324**(1–2), 71–79 (2008)
118. D.H. Napper, Steric stabilization. J. Colloid Interface Sci. **58**(2), 390–407 (1977)
119. A.-M. Sung, I. Piirma, Electrosteric stabilization of polymer colloids. Langmuir **10**(5), 1393–1398 (1994)
120. B.S.M. Claudio, L. De Castro, Nanoparticles from mechanical attrition. Synth. Funct. Surf. Treat. Nanoparticles, 1–14 (2002)
121. Y. Lu, S. Guan, L. Hao, H. Yoshida, *Review on the Photocatalyst Coatings of TiO2: Fabrication by Mechanical Coating Technique and Its Application*, (2015), pp. 425–464
122. M. Boutonnet Kizling, S.G. Järås, Appl. Catal. A **147**, 1–21 (1996)
123. Z.R. Ismagilov, O.Y. Podyacheva, O.P. Solonenko, V.V. Pushkarev, V.I. Kuz'min, V.A. Ushakov, N.A. Rudina, Catal. Today **51**, 411–417 (1999)
124. C.-J. Liu, G.P. Vissokov, B.W.L. Jang, Catal. Today **72**, 173–184 (2002)
125. H. Shim, J. Phillips, I.M. Fonseca, S. Carabinerio, Appl. Catal. A **237**, 41–51 (2002)
126. S. Hinokuma, K. Murakami, K. Uemura, M. Matsuda, K. Ikeue, N. Tsukahara, M. Machida, Top. Catal. **52**, 2108–2111 (2009)
127. S. Hinokuma, M. Okamoto, E. Ando, K. Ikeue, M. Machida, Catal. Today **175**, 593–597 (2011)
128. S. Hinokuma, M. Okamoto, E. Ando, K. Ikeue, M. Machida, Bull. Chem. Soc. Jpn. **85**, 144–149 (2012)
129. S. Hinokuma, Y. Katsuhara, E. Ando, K. Ikeue, M. Machida, Catal. Today **201**, 92–97 (2013)
130. S. Hinokuma, H. Fujii, Y. Katsuhara, K. Ikeue, M. Machida, Cat. Sci. Technol. **4**, 2990–2996 (2014)
131. S. Hinokuma, H. Kogami, N. Yamashita, Y. Katsuhara, K. Ikeue, M. Machida, Catal. Commun. **54**, 81–85 (2014)
132. S. Hinokuma, N. Yamashita, Y. Katsuhara, H. Kogami, M. Machida, Cat. Sci. Technol. **5** (2015). https://doi.org/10.1039/c1035cy00370a
133. Y. Agawa, S. Endo, M. Matsuura, Y. Ishii, ECS Trans. **50**, 1271–1276 (2012)
134. T. Fujitani, I. Nakamura, Angew. Chem. Int. Ed. **50**, 10144–10147 (2011)
135. K. Qadir, S.H. Kim, S.M. Kim, H. Ha, J.Y. Park, J. Phys, Chem. C **116**, 24054–24059 (2012)
136. S.H. Kim, C.H. Jung, N. Sahu, D. Park, J.Y. Yun, H. Ha, J.Y. Park, Appl. Catal. A **454**, 53–58 (2013)
137. T. Yoshitake, Y. Nakagawa, A. Nagano, R. Ohtani, H. Setoyama, E. Kobayashi, K. Sumitani, Y. Agawa, K. Nagayama, Jpn. J. Appl. Phys. **49**, 015503 (2010)

138. K. Hanada, T. Yoshida, Y. Nakagawa, T. Yoshitake, Jpn. J. Appl. Phys. **49**, 125503 (2010)
139. C. Qin, S. Coulombe, Mater. Lett. **60**, 1973–1976 (2006)
140. A.V. Stanishevsky, E.L. Tochitsky, J. Wide Bandgap Mater. **4**, 297–310 (1996)
141. A.S. Chaus, T.N. Fedosenko, A.V. Rogachev, Ľ. Čaplovič, Diamond Relat. Mater. **42**, 64–70 (2014)
142. B. Naik, S.M. Kim, C.H. Jung, S.Y. Moon, S.H. Kim, J.Y. Park, Adv. Mater. Interfaces **1**, 201300018 (2014)
143. S. Hinokuma, S. Misumi, H. Yoshida, M. Machida, Cat. Sci. Technol. **5**, 4249 (2015). https://doi.org/10.1039/c5cy00636h
144. A. Albanese, P.S. Tang, W.C.W. Chan, The effect of nanoparticle size, shape, and surface chemistry on biological systems. Annu. Rev. Biomed. Eng. **14**, 1–16 (2012)
145. N. Subcommittee of the National Science and T. Council, "National Nanotechnology Initiative Supplement to the President's 2019 Budget," no. August 2018, p. 24, (2019)
146. P. Buffat, J.P. Borel, Size effect on the melting temperature of gold particles. Phys. Rev. A **13**(6), 2287–2298 (1976)
147. J. Jortner, Cluster size effects. Zeitschrift für Phys. D Atoms, Mol. Clust. **24**(3), 247–275 (1992)
148. C.D. Didomenico, M. Lintz, L.J. Bonassar, Molecular transport in articular cartilage - What have we learned from the past 50 years? Nat. Rev. Rheumatol. **14**(7), 393–403 (2018)
149. S.D. Perrault, C. Walkey, T. Jennings, H.C. Fischer, W.C.W. Chan, Mediating tumor targeting efficiency of nanoparticles through design. Nano Lett. **9**(5), 1909–1915 (2009)
150. K. R. Backe, P. Skalle, O. B. Lile, *Shrinkage of Oil Well Cement Slurries*
151. P. J. Boul, P. M. Ajayan, *Nanotechnology Research and Development in Upstream Oil and Gas*, vol. 1901216, (2020)
152. Y. Bu, X. Hou, C. Wang, J. Du, Effect of colloidal nanosilica on early-age compressive strength of oil well cement stone at low temperature. Constr. Build. Mater. **171**, 690–696 (2018)
153. I. Panas, A. Martinelli, A. Matic, Accelerating effects of colloidal nano-silica for beneficial calcium – silicate – hydrate formation in cement. Chemical Physics Letters **392**, 242–248 (2004)
154. X. Pang, P. J. Boul, W. C. Jimenez, *IADC / SPE 168037 Nanosilicas as Accelerators in Oilwell Cementing at Low Temperatures*, no. March, pp. 4–6, (2014)
155. D. Enescu, M.A. Cerqueira, P. Fucinos, L.M. Pastrana, Recent advances and challenges on applications of nanotechnology in food packaging. A literature review. Food Chem. Toxicol **134**(May), 110814 (2019)
156. H. Mu, H. Gao, H. Chen, F. Tao, X. Fang, L. Ge, A nanosised oxygen scavenger : Preparation and antioxidant application to roasted sunflower seeds and walnuts. Food Chem. **136**(1), 245–250 (2013)
157. G.O. Noonan, A.J. Whelton, D. Carlander, T.V. Duncan, Measurement Methods to Evaluate Engineered Nanomaterial Release from Food Contact Materials. Comprehensive Reviews in Food Science and Food Safety **13**, 679–692 (2014)
158. Z. Zhang et al., NanoImpact Development of a standardized food model for studying the impact of food matrix effects on the gastrointestinal fate and toxicity of ingested nanomaterials. NanoImpact **13**, 13–25 (2019)
159. C.G. Otoni, P.J.P. Espitia, R.J. Avena-bustillos, T.H. Mchugh, Trends in antimicrobial food packaging systems: Emitting sachets and absorbent pads. FRIN **83**, 60–73 (2016)
160. H. Chung, M. Yu, Q.P. Nguyen, J. Pet. Sci. Eng. Nanotechnol. Oil Field Appl. Challenges. Impact **157**, 1160–1169 (2017)
161. A. Sánchez Jiménez et al., Safe(r) by design implementation in the nanotechnology industry. NanoImpact **20**(July) (2020)